

## *Cover Page for Supporting Information*

### ***Manuscript Title:***

**2-Butene Tetraanion Bridged Dinuclear Samarium(III) Complexes via Sm(II)-Mediated Reduction of Electron-Rich Olefins**

### ***Authors:***

Yu Zheng,<sup>a</sup> Chang-Su Cao,<sup>b</sup> Wangyang Ma,<sup>a</sup> Tianyang Chen,<sup>a</sup> Botao Wu,<sup>a</sup> Chao Yu,<sup>a</sup> Zhe Huang,<sup>a</sup> Jianhao Yin,<sup>a</sup> Han-Shi Hu,<sup>\*,b</sup> Jun Li,<sup>b,c</sup> Wen-Xiong Zhang,<sup>\*,a</sup> and Zhenfeng Xi<sup>a</sup>

### ***Affiliations:***

<sup>a</sup> Beijing National Laboratory for Molecular Sciences (BNLMS), Key Laboratory of Bioorganic Chemistry and Molecular Engineering of Ministry of Education, College of Chemistry, Peking University, Beijing 100871, China

<sup>b</sup> Department of Chemistry and Key Laboratory of Organic Optoelectronics & Molecular Engineering of Ministry of Education, Tsinghua University, Beijing 100084, China

<sup>c</sup> Department of Chemistry, Southern University of Science and Technology, Shenzhen 518055, China

### ***Contents:***

<b>1) Experimental Details and Characterization Data</b>	<b>S2</b>
<b>2) Copies of <sup>1</sup>H NMR and <sup>13</sup>C NMR Spectra of All New Compounds</b>	<b>S7</b>
<b>3) X-ray Crystallographic Studies</b>	<b>S14</b>
<b>4) UV-Vis Spectrum and Magnetic Susceptibility of 2</b>	<b>S23</b>
<b>5) Details of DFT Calculations</b>	<b>S24</b>
<b>5.1 Calculations on the Structures of 2 and 3</b>	<b>S24</b>
<b>5.2 Calculations on the Proposed Mechanisms for the Formation of 2</b>	<b>S40</b>
<b>6) References</b>	<b>S43</b>

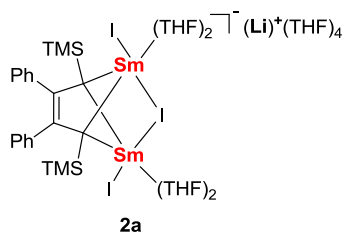
## 1) Experimental Details and Characterization Data

Unless otherwise noted, all reactions were conducted under slightly positive dry nitrogen pressure using standard Schlenk line techniques or under an argon atmosphere in a Vigor (SG 1200/750TS-F) glovebox. The oxygen and moisture concentrations in the glovebox atmosphere were monitored by an O<sub>2</sub>/H<sub>2</sub>O Combi-Analyzer to ensure both were always below 1 ppm. Unless otherwise noted, all starting materials were commercially available and were used without further purification. Solvents were purified by an Mbraun SPS-800 Solvent Purification System and dried over fresh Na chips in a glovebox. Organometallic samples for NMR spectroscopic measurements were prepared in a glovebox by the use of J. Young valve NMR tubes (Wilmad 528-JY). <sup>1</sup>H and <sup>13</sup>C NMR spectra were recorded on a Bruker ARX400 spectrometer (FT, 400 MHz for <sup>1</sup>H; 100 MHz for <sup>13</sup>C) at ambient temperature, unless otherwise noted. <sup>1</sup>H and <sup>13</sup>C NMR spectra were reported with reference to solvent resonances of *d*<sup>8</sup>-THF at 1.73 ppm (for <sup>1</sup>H NMR spectra) and 25.37 ppm (for <sup>13</sup>C NMR spectra). IR spectra were recorded on a BRUKER LAPHIA II spectrometer. UV/visible spectroscopy was performed on samples in sealed 10 mm path length cuvettes on an Agilent Technologies Cary 60 UV/Vis spectrophotometer. Magnetic susceptibility measurement was performed using a Quantum Design MPMS-XL7 SQUID magnetometer on polycrystalline sample.

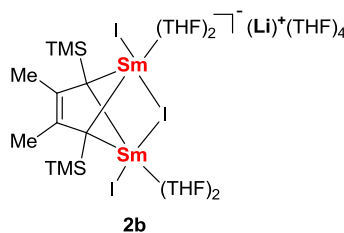
**Note:** Because of the high sensitivity of these complexes to air and moisture and also high lability of coordinated THF molecules, some samples easily decompose or lost weight even in triple layers of tin boats and thus their elemental analysis data are not well consistent with the calculated values and/or are not given.

### *General Procedure for the Synthesis of 2a-c*

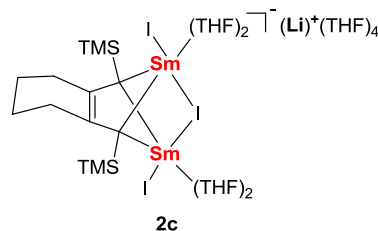
In the glovebox, SmI<sub>2</sub>(THF)<sub>2</sub> powder (548.4 mg, 1.0 mmol) was dissolved in THF solution (5 mL) in a 25 mL flask. Then the THF solution (3 mL) of 1,4-dilithio-1,3-butadiene **1** (0.5 mmol) was added dropwise into the above solution and stirred at room temperature for 3 h. During the addition of THF solution of **1**, the color of reaction mixture changed to yellow-brown gradually. After that, the solvent was removed under reduced pressure. The residue was washed with toluene for several times, and then was dried under reduced pressure to give dark brown solids. The single crystals of **2a** and **2c** suitable for X-ray analysis could be obtained by volatilization of THF/Et<sub>2</sub>O/Hexane solution at -20 °C and room temperature for 2 days, respectively.



**2a:** Dark brown solid (581.0 mg, 0.36 mmol, 72% isolated yield).  $^1\text{H}$  NMR (400 MHz,  $d^8$ -THF)  $\delta$   $-0.53$  (s, 18H,  $\text{Me}_3\text{Si}$ ),  $5.16$  (d,  $J = 7.6$  Hz, 4H, Ph),  $6.11$  (t,  $J = 7.3$  Hz, 4H, Ph),  $6.51$  (d,  $J = 7.1$  Hz, 2H, Ph).  $^{13}\text{C}$  NMR (100 MHz,  $d^8$ -THF)  $\delta$   $-6.8$  ( $\text{Me}_3\text{Si}$ ),  $26.4$  ( $\beta\text{-CH}_2$ , THF),  $68.5$  ( $\alpha\text{-CH}_2$ , THF),  $122.2$  (Ph),  $124.2$  (Ph),  $127.6$  (Ph),  $131.8$  (Ph),  $155.8$  ( $\beta\text{-C}$ ). The  $\alpha\text{-C}$  atoms are not observed due to the coupling with two samarium(III) ions. Anal. Calcd for  $\text{C}_{54}\text{H}_{92}\text{I}_3\text{LiO}_8\text{Si}_2\text{Sm}_2$ : C, 40.19; H, 5.75. Found: C, 40.19; H, 5.82.



**2b:** Dark brown solid (657.7 mg, 0.44 mmol, 88% isolated yield).  $^1\text{H}$  NMR (400 MHz,  $d^8$ -THF)  $\delta$   $-0.25$  (s, 18H,  $\text{Me}_3\text{Si}$ ),  $2.48$  (s, 6H,  $\text{CH}_3$ ).  $^{13}\text{C}$  NMR (100 MHz,  $d^8$ -THF)  $\delta$   $-7.6$  ( $\text{Me}_3\text{Si}$ ),  $26.4$  ( $\beta\text{-CH}_2$ , THF),  $27.6$  ( $\text{CH}_3$ ),  $69.4$  ( $\alpha\text{-CH}_2$ , THF),  $123.3$  ( $\beta\text{-C}$ ). The  $\alpha\text{-C}$  atoms are not observed due to the coupling with two samarium(III) ions. Anal. Calcd for  $\text{C}_{44}\text{H}_{88}\text{I}_3\text{LiO}_8\text{Si}_2\text{Sm}_2$ : C, 35.48; H, 5.95. Found: C, 35.93; H, 5.57.



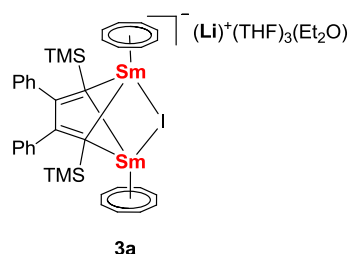
**2c:** Dark brown solid (713.9 mg, 0.47 mmol, 94% isolated yield).  $^1\text{H}$  NMR (400 MHz,  $d^8$ -THF)  $\delta$   $-0.26$  (s, 18H,  $\text{Me}_3\text{Si}$ ),  $1.49$  (s, 4H,  $\beta\text{-CH}_2$ ),  $2.46$  (s, 4H,  $\alpha\text{-CH}_2$ ).  $^{13}\text{C}$  NMR (100 MHz,  $d^8$ -THF)  $\delta$   $-7.2$  ( $\text{Me}_3\text{Si}$ ),  $25.5$  ( $\beta\text{-CH}_2$ ),  $26.4$  ( $\beta\text{-CH}_2$ , THF),  $39.3$  ( $\alpha\text{-CH}_2$ ),  $69.3$  ( $\alpha\text{-CH}_2$ , THF),  $125.5$  ( $\beta\text{-C}$ ). The  $\alpha\text{-C}$  atoms are not observed due to the coupling with two samarium(III) ions.

The elemental analysis data are not well consistent with the calculated values due to the high sensitivity of these complexes to air and moisture or high lability of coordinated solvents.

### Procedure for the Synthesis of 3a

In the glovebox, **2a** was prepared *in situ* and used for further reaction in one-pot without post-procedure.  $\text{SmI}_2(\text{THF})_2$  powder (274.2 mg, 0.5 mmol) was dissolved in THF solution (5 mL) in a 25 mL flask. The THF solution (3 mL) of 1,4-dilithio-1,3-butadiene **1a** (90.6 mg, 0.25 mmol) was added dropwise into the above solution and stirred at room temperature for 3 h. Then a THF solution ( $\sim 5$  mL) of cyclooctatetraene (26.1 mg, 0.25 mmol) was added to the above solution and stirred at room temperature for 3 h. The formation of alkyne  $\text{PhC}\equiv\text{CTMS}$  could be confirmed by NMR and GC-MS. The solvent THF was then removed under reduced pressure and the residue was extracted with cooled toluene for three times,  $\text{LiI}$  was filtered and the filtrate was removed under reduced pressure to give dark purple solids. Hexane ( $\sim 5$  mL) was added to the residue. The mixture was stored at  $-20^\circ\text{C}$  overnight. Then the yellow

supernatant was removed and the dark purple residue was washed with cold hexane (~5 mL). The residue was then dried under vacuum. The residue was then extracted with ether for several times, and the volatiles of the filtrate were removed under reduced pressure to give brown solids. The single crystals suitable for X-ray analysis could be grown from THF/Et<sub>2</sub>O/Hexane solution of **3a** at –20 °C for 3 days. The residual solid was dissolved in THF and 0.1 mL DME was added. The mixture was stored at –20 °C overnight and the single crystals [SmI<sub>2</sub>(DME)<sub>2</sub>(THF)] could be grown at –20 °C for 3 days which was confirmed by X-ray analysis.

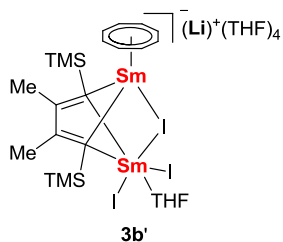


**3a**: Dark red solid, (83.9 mg, 0.065 mmol, 26% isolated yield based on the starting material of **2a**, the maximum yield is 50%). <sup>1</sup>H NMR (400 MHz, *d*<sup>8</sup>-THF)  $\delta$  –0.53 (s, 18H, Me<sub>3</sub>Si), 7.13–7.20 (m, 6H, Ph), 7.97 (d, *J* = 6.6 Hz, 4H, Ph), 9.21 (s, 16H, C<sub>8</sub>H<sub>8</sub>). <sup>13</sup>C NMR (100 MHz, *d*<sup>8</sup>-THF)  $\delta$  3.7 (Me<sub>3</sub>Si), 25.3 ( $\beta$ -CH<sub>2</sub>, THF), 67.4 ( $\alpha$ -CH<sub>2</sub>, THF), 83.1 (C<sub>8</sub>H<sub>8</sub>), 125.4 (Ph), 127.4 (Ph), 128.5 (Ph), 139.8 (Ph), 167.9 ( $\beta$ -C). The  $\alpha$ -C atoms are not observed due to

the coupling with two samarium(III) ions. The elemental analysis data are not well consistent with the calculated values due to the high sensitivity of this complex to air and moisture or high lability of coordinated solvents.

### Procedure for the Synthesis of **3b'**

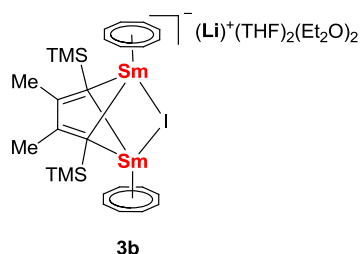
In the glovebox, a THF solution (5 mL) of cyclooctatetraene (10.4 mg, 0.10 mmol) was added to the THF solution of **2b** (142.5 mg, 0.096 mmol) and the mixture was stirred at room temperature for 3 h. Then the solvent THF was removed under reduced pressure and the residue was washed with hexane for three times, and the solid was recrystallized in THF/hexane at –20 °C overnight. The black crystalline solid **3b'** was obtained after removing the mother solution and washing with hexane for 3 times.



**3b'**: Black crystalline solid (67.6 mg, 0.049 mmol, 51% crystal yield). <sup>1</sup>H NMR (400 MHz, *d*<sup>8</sup>-THF)  $\delta$  –2.13 (s, 18H, Me<sub>3</sub>Si), 2.98 (s, 6H, CH<sub>3</sub>), 10.96 (s, 8H, C<sub>8</sub>H<sub>8</sub>). <sup>13</sup>C NMR (100 MHz, *d*<sup>8</sup>-THF)  $\delta$  –0.5 (Me<sub>3</sub>Si), 25.9 (CH<sub>3</sub>), 26.4 ( $\beta$ -CH<sub>2</sub>, THF), 68.3 ( $\alpha$ -CH<sub>2</sub>, THF), 84.3 (C<sub>8</sub>H<sub>8</sub>), 176.3 ( $\beta$ -C). The  $\alpha$ -C atoms are not observed due to the coupling with two samarium(III) ions. Anal. Calcd for C<sub>40</sub>H<sub>72</sub>I<sub>3</sub>LiO<sub>5</sub>Si<sub>2</sub>Sm<sub>2</sub>: C, 34.88; H, 5.27. Found: C, 34.95; H, 5.33.

### Procedure for the Synthesis of **3b**

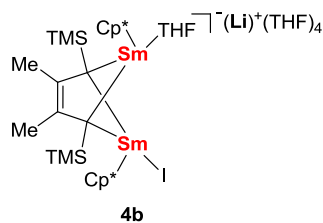
In the glovebox, the black crystalline solid **3b'** (142.1 mg, 0.103 mmol) was dissolved in THF solution (5 mL) in a 25 mL Schlenk tube and removed from the glovebox. The tube was stirred at 80 °C for 12 h. After the stirring is finished, the solvent THF was removed under reduced pressure and the residue was washed by hexane for three times to remove the alkyne  $\text{MeC}\equiv\text{CTMS}$ , which was confirmed by NMR and GC-MS. The residue was then extracted with ether for several times, and the volatiles of the filtrate were removed under reduced pressure to give brown solids which was recrystallized by the mixture of  $\text{Et}_2\text{O}$ /hexane. The single crystals suitable for X-ray analysis could be grown from  $\text{Et}_2\text{O}$ /Hexane solution at  $-20\text{ }^\circ\text{C}$  for 1 day. The black crystalline solid **3b** was obtained after removing the mother liquor and washing with hexane for 3 times. The residual solid was dissolved in THF and 0.1 mL DME was added. The mixture was stored at  $-20\text{ }^\circ\text{C}$  overnight and the single crystals  $[\text{SmI}_2(\text{DME})_2(\text{THF})]$  could be grown at  $-20\text{ }^\circ\text{C}$  for 3 days which was confirmed by X-ray analysis.



**3b**: Black solid (66.9 mg, 0.024 mmol, 23% crystal yield based on the starting material of **3b'**, the maximum yield is 50%).  $^1\text{H}$  NMR (400 MHz,  $d^8$ -THF)  $\delta$   $-0.23$  (s, 18H,  $\text{Me}_3\text{Si}$ ),  $2.47$  (s, 6H,  $\text{CH}_3$ ),  $8.98$  (s, 16H,  $\text{C}_8\text{H}_8$ ).  $^{13}\text{C}$  NMR (100 MHz,  $d^8$ -THF)  $\delta$   $2.8$  ( $\text{Me}_3\text{Si}$ ),  $25.9$  ( $\text{CH}_3$ ),  $82.9$  ( $\text{C}_8\text{H}_8$ ),  $167.5$  ( $\beta\text{-C}$ ). The  $\alpha\text{-C}$  atoms are not observed due to the coupling with two samarium(III) ions. The elemental analysis data are not well consistent with the calculated values due to the high sensitivity of this complex to air and moisture or high lability of coordinated solvents.

### Procedure for the Synthesis of **4b**

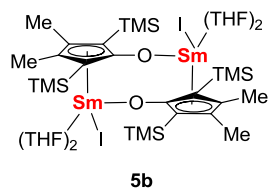
In the glovebox, complex **2b** was prepared *in situ* and used for further reaction in one-pot without post-procedure.  $\text{SmI}_2(\text{THF})_2$  powder (219.4 mg, 0.40 mmol) was dissolved in THF solution (5 mL) in a 25 mL flask. Then the THF solution (3 mL) of 1,4-dilithio-1,3-butadiene **1b** (47.7 mg, 0.20 mmol) was added dropwise into the above solution and stirred at room temperature for 3 h. Then a THF solution ( $\sim 5$  mL) of  $\text{Cp}^*\text{Li}$  (62.6 mg, 0.44 mmol,  $\text{Cp}^* = \text{pentamethylcyclopentadienyl}$ ) was added to the above solution and stirred at room temperature for 12 h. Then the solvent THF was removed under reduced pressure and the residue was extracted with toluene for three times to remove  $\text{LiI}$  and then washed with hexane for three times. The residue was then dried under vacuum to give yield solid. The single crystals suitable for X-ray analysis could be grown from THF/Hexane solution of **4b** at room temperature overnight.



**4b:** Yellow solid (226.6 mg, 0.175 mmol, 88% yield).  $^1\text{H}$  NMR (400 MHz,  $d^8$ -THF)  $\delta$  -3.40 (s, 18H,  $\text{Me}_3\text{Si}$ ), -1.34 (s, 6H,  $\text{CH}_3$ ), 2.57 (30H,  $\text{Me}_5\text{C}_5$ ).  $^{13}\text{C}$  NMR (100 MHz,  $d^8$ -THF)  $\delta$  -10.0 ( $\text{Me}_3\text{Si}$ ), 21.0 ( $\text{Me}_5\text{C}_5$ ), 24.5 ( $\text{CH}_3$ ), 26.4 ( $\beta$ - $\text{CH}_2$ , THF), 68.4 ( $\alpha$ - $\text{CH}_2$ , THF), 102.4 ( $\beta$ -C), 112.6 ( $\text{Me}_5\text{C}_5$ ). The  $\alpha$ -C atoms are not observed due to the coupling with two samarium(III) ions. Anal. Calcd for  $\text{C}_{52}\text{H}_{94}\text{LiO}_5\text{Si}_2\text{Sm}_2$ : C, 48.41; H, 7.34. Found: C, 47.83; H, 7.30.

### Procedure for the Synthesis of 5b

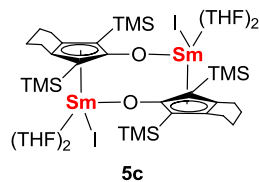
In the glovebox, the complex **2b** (107.8 mg, 0.07 mmol) was dissolved in THF solution (2 mL) in a 25 mL flask. Then the THF solution (2 mL) of  $\text{Mo}(\text{CO})_6$  (22.9 mg, 0.10 mmol) was added dropwise into the above solution and stirred at room temperature for 2 h. Then the solvent was concentrated to about 1 mL under reduced pressure and the single crystals **5b** suitable for X-ray analysis could be grown at room temperature overnight. Crystalline complex **5b** is difficult to dissolve in THF and other solvents, and no NMR signal was observed.



**5b:** Red crystal (41.2 mg, 0.028 mmol, 38% yield based on Sm). The elemental analysis data are not well consistent with the calculated values due to the high sensitivity of this complex to air and moisture or high lability of coordinated solvents. IR ( $\text{cm}^{-1}$ ): 469 (w), 620 (w), 646 (m), 681 (w), 749 (m), 832 (vs), 1019 (m), 1112 (w), 1240 (m), 1311 (w), 1371 (s), 1927 (w), 2949 (w).

### Procedure for the Synthesis of 5c

In the glovebox, the complex **2c** (122.2 mg, 0.08 mmol) was dissolved in THF solution (2 mL) in a 25 mL flask. Then the THF solution (2 mL) of  $\text{Mo}(\text{CO})_6$  (25.5 mg, 0.09 mmol) was added dropwise into the above solution and stirred at room temperature for 2 h. Then the solvent was concentrated to about 1 mL under reduced pressure and the single crystals **5c** suitable for X-ray analysis could be grown at room temperature overnight. Crystalline complex **5c** is difficult to dissolve in THF and other solvents and no NMR signal was observed.



**5c:** Red crystal (54.5 mg, 0.035 mmol, 44% yield based on Sm). Anal. Calcd for  $\text{C}_{54}\text{H}_{100}\text{I}_2\text{O}_8\text{Si}_4\text{Sm}_2$ : C, 42.00; H, 6.54. Found: C, 41.61; H, 6.46. IR ( $\text{cm}^{-1}$ ): 476 (w), 497 (w), 617 (w), 681 (w), 749 (m), 831 (vs), 955 (w), 1015 (m), 1108 (w), 1242 (m), 1313 (m), 1370 (s), 1924 (w), 2928 (w).

## 2) Copies of $^1\text{H}$ NMR and $^{13}\text{C}$ NMR Spectra of All New Compounds

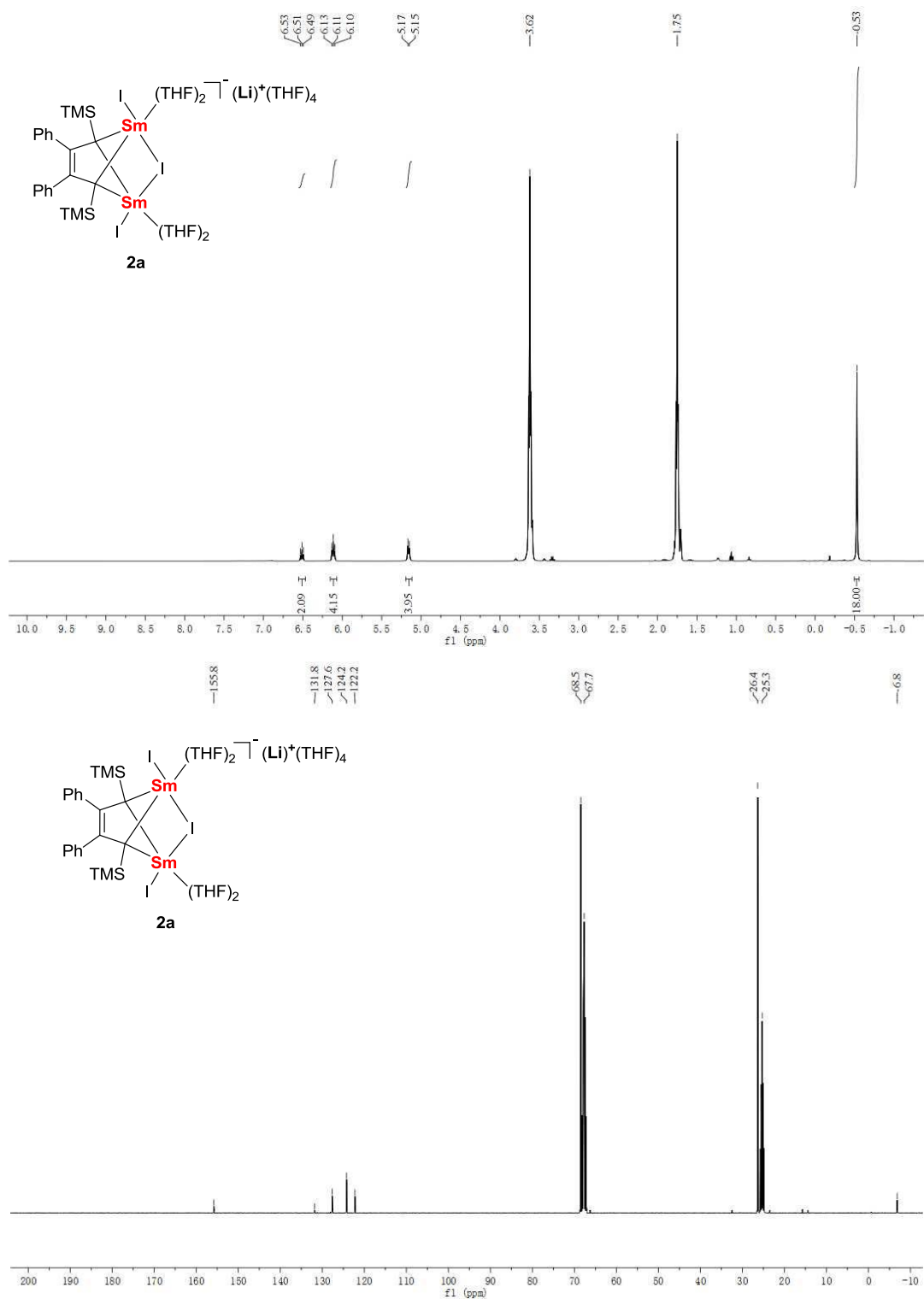


**Figure S1.**  $^1\text{H}$  NMR and  $^{13}\text{C}$  NMR spectra of **2a** (25 °C, 400 MHz,  $d^8$ -THF).

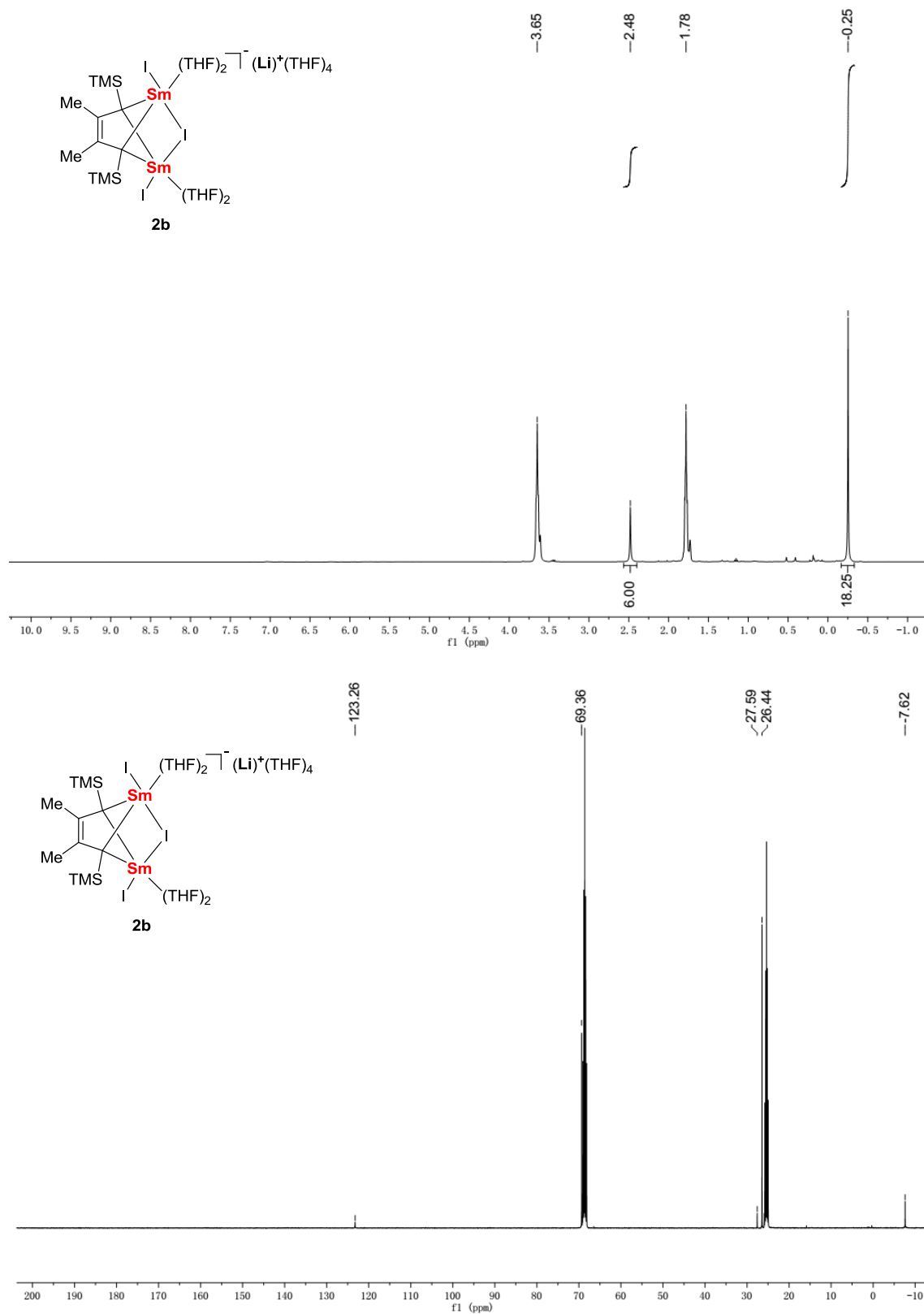


**Figure S2.** <sup>1</sup>H NMR and <sup>13</sup>C NMR spectra of **2b** (25 °C, 400 MHz, *d*<sup>8</sup>-THF).



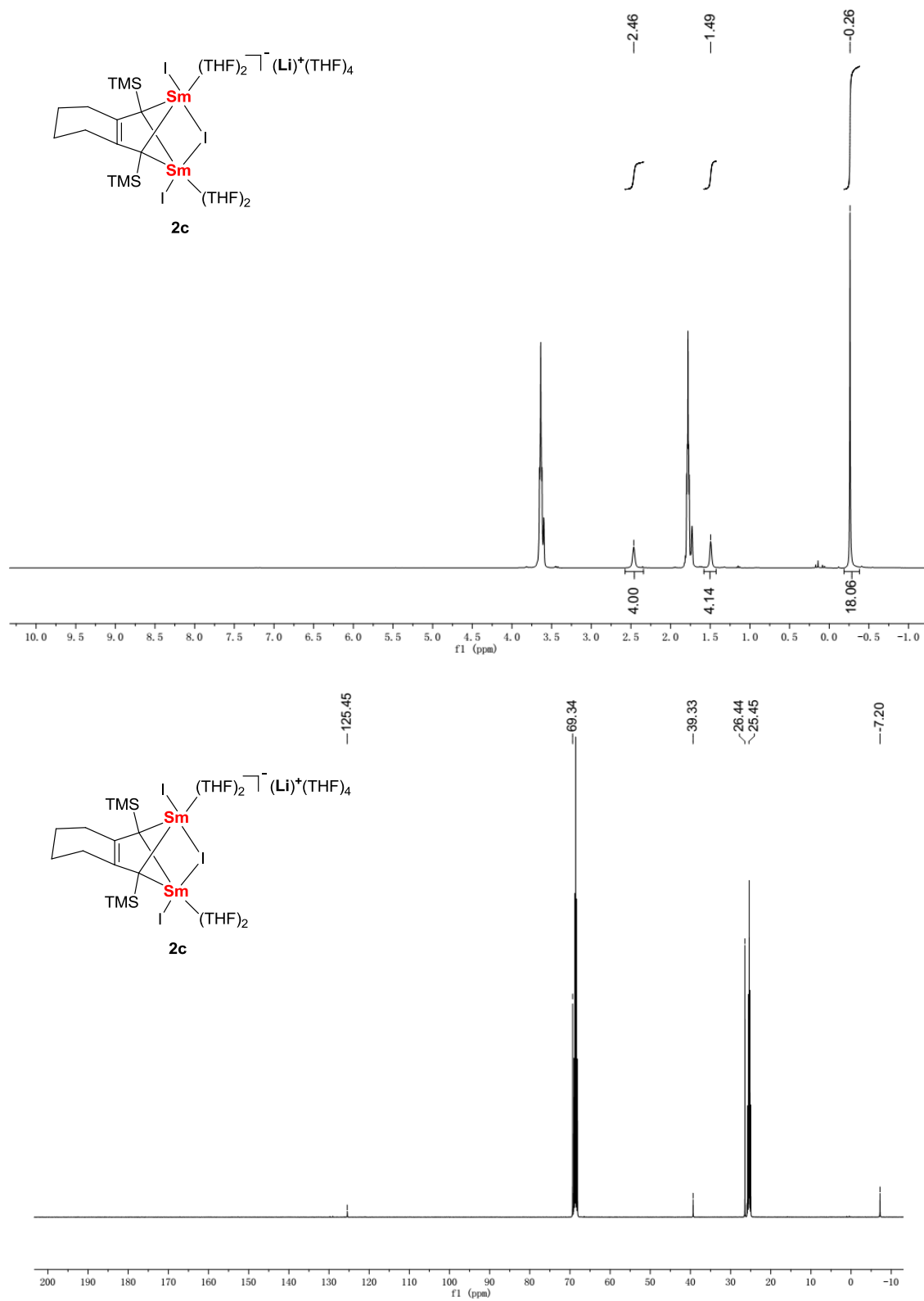


**Figure S3.** <sup>1</sup>H NMR and <sup>13</sup>C NMR spectra of **2c** (25 °C, 400 MHz, *d*<sup>8</sup>-THF).

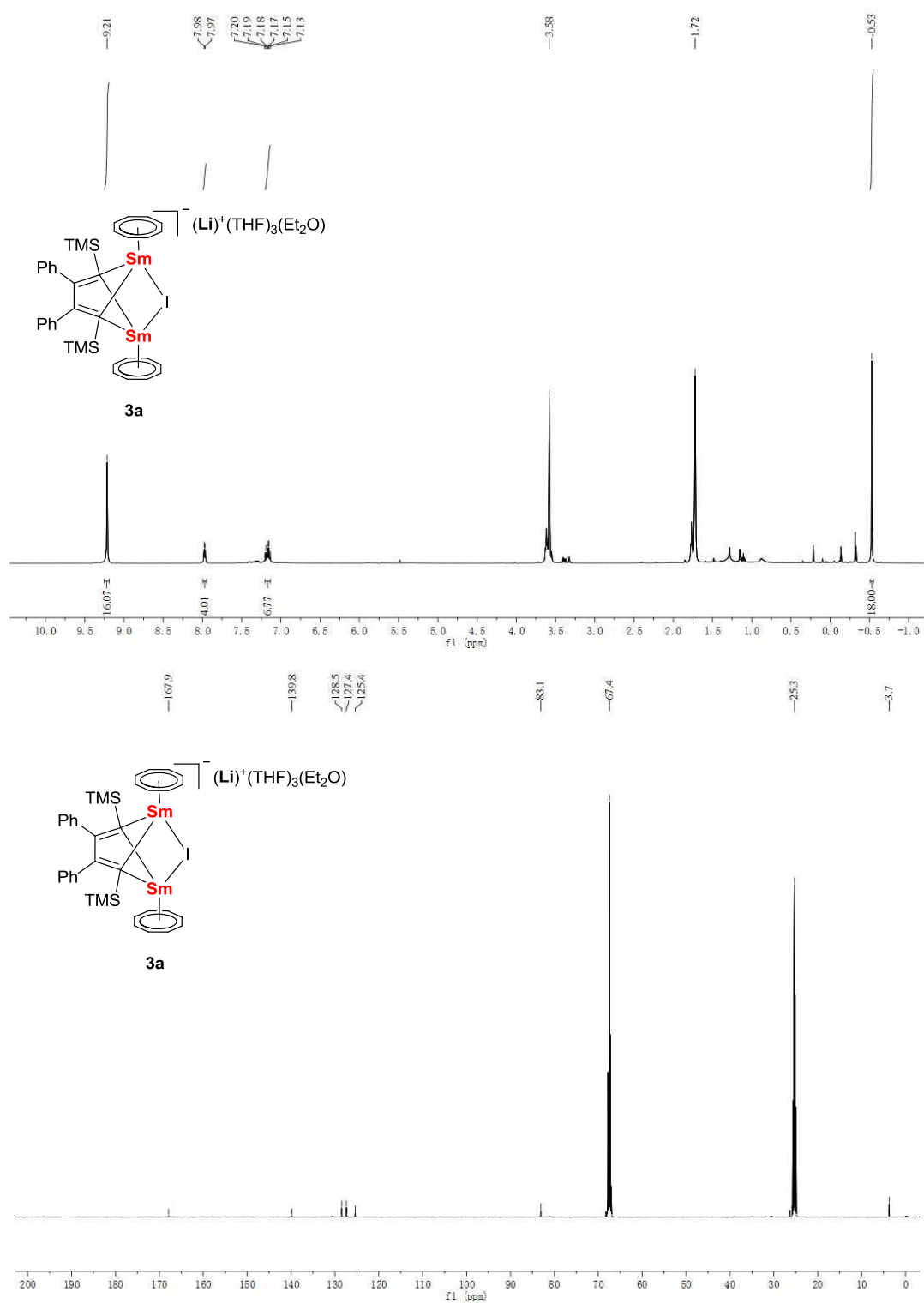


**Figure S4.**  $^1\text{H}$  NMR and  $^{13}\text{C}$  NMR spectra of **3a** (25 °C, 400 MHz,  $d^8$ -THF).

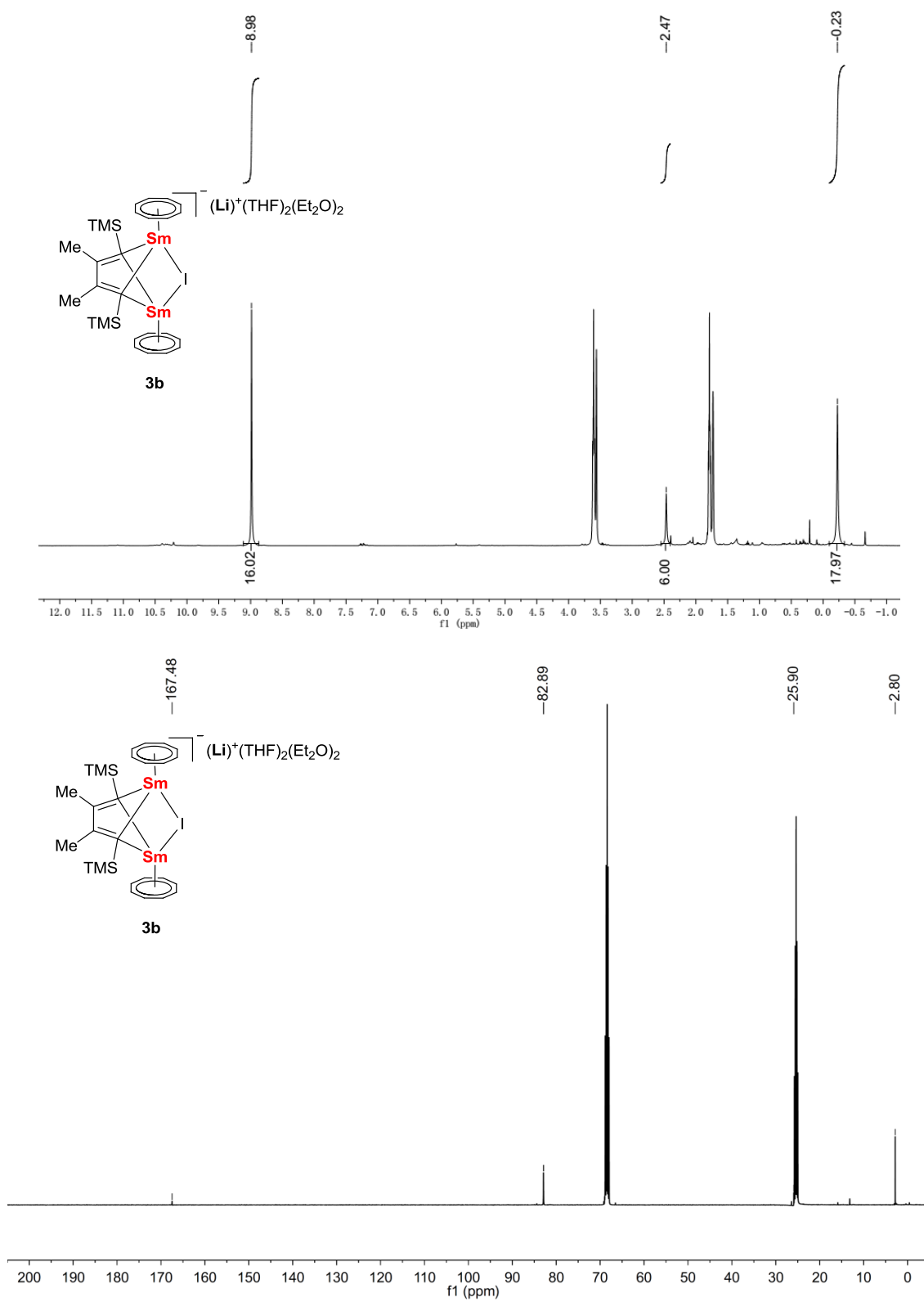


**Figure S5.** <sup>1</sup>H NMR and <sup>13</sup>C NMR spectra of **3b** (25 °C, 400 MHz, *d*<sup>8</sup>-THF).

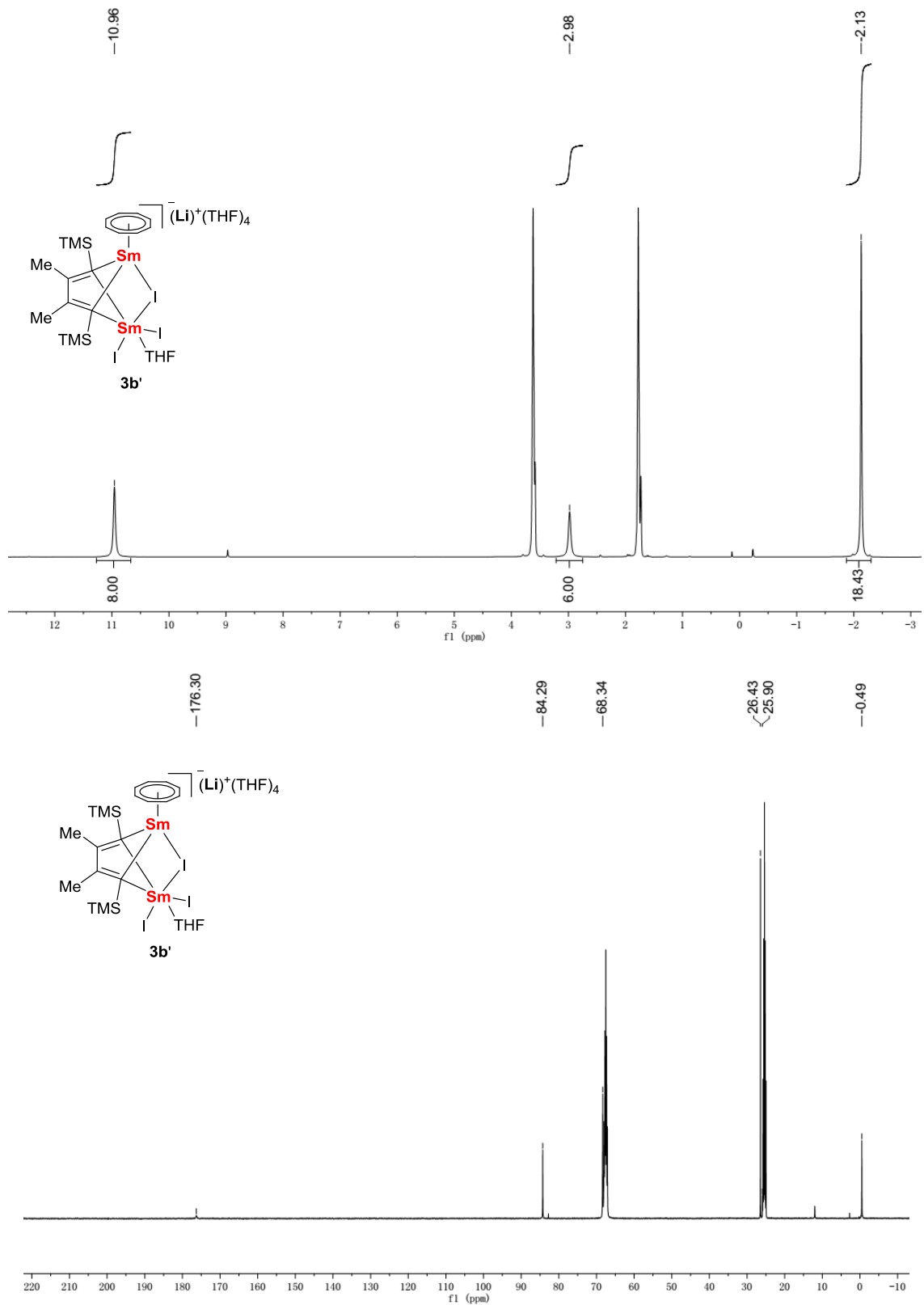


**Figure S6.** <sup>1</sup>H NMR and <sup>13</sup>C NMR spectra of **3b'** (25 °C, 400 MHz, *d*<sup>8</sup>-THF).

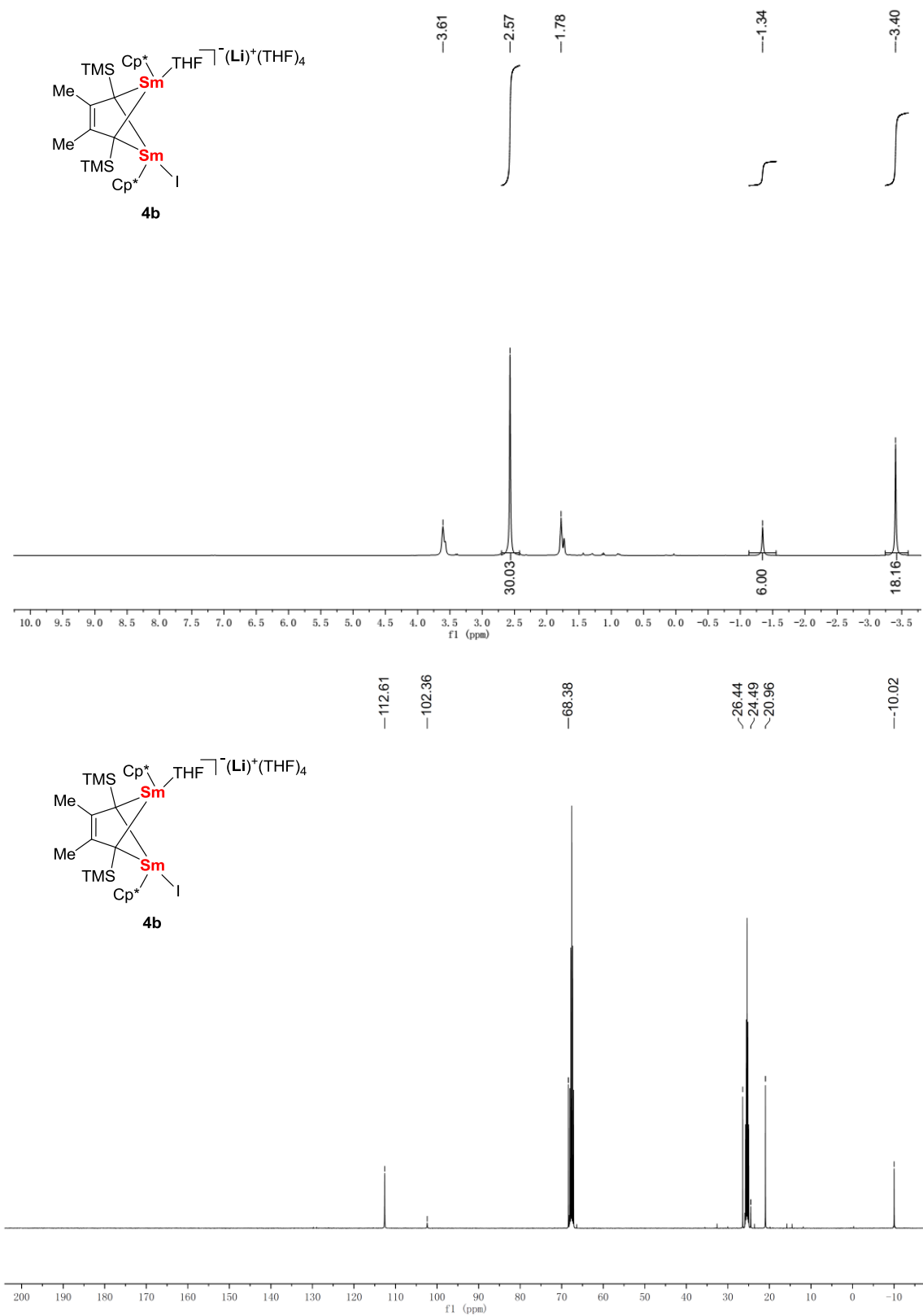


**Figure S7.**  $^1\text{H}$  NMR and  $^{13}\text{C}$  NMR spectra of **4b** (25 °C, 400 MHz,  $d^8$ -THF).

### 3) X-ray Crystallographic Studies

The single crystals of **2a•THF**, **2c**, **3a**, **3b**, **3b'**, **4b**, **5b•THF** and **5c•THF** suitable for X-ray analysis were grown as described in the experimental section. The crystals were wrapped in mineral oil and then were frozen in low temperature. Data collections were performed at 100 or 180 K on a XtaLAB PRO 007HF: Kappa single diffractometer, using graphite-monochromated Mo K $\alpha$  radiation ( $\lambda = 0.71073$  Å). Using Olex2,<sup>1</sup> the structures were solved with Superflip<sup>2</sup> structure solution program using Charge Flipping or ShelXS-97<sup>3</sup> structure solution program using Direct Methods and refined with the ShelXL<sup>4</sup> refinement package using Least Squares minimization. Refinement was performed on  $F^2$  anisotropically for all the non-hydrogen atoms by the full-matrix least-squares method. The hydrogen atoms were placed at the calculated positions and were included in the structure calculation without further refinement of the parameters. Crystal data, data collection and processing parameters are summarized in Table S8-S15. Crystallographic data have been deposited with the Cambridge Crystallographic Data Centre as supplementary publication nos. CCDC 1982325 (**2a•THF**), CCDC 1982038 (**2c**), CCDC 1576765 (**3a**), CCDC 1982066 (**3b**), CCDC 1982074 (**3b'**), CCDC 1982078 (**4b**) CCDC 1982080 (**5b•THF**) and CCDC 1982083 (**5c•THF**). Copies of these data can be obtained free of charge from the Cambridge Crystallographic Data Centre via [www.ccdc.cam.ac.uk/data\\_request/cif](http://www.ccdc.cam.ac.uk/data_request/cif). The thermal ellipsoid plot in the Figures were drawn by Ortep-3 v1.08.<sup>5</sup>

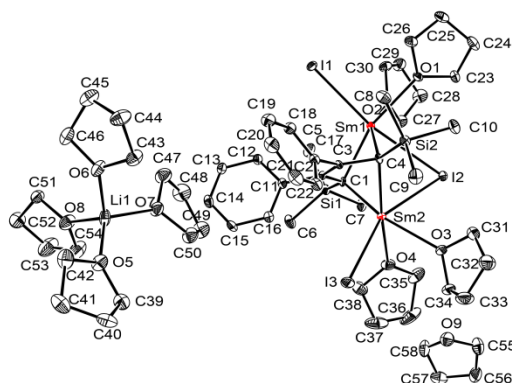


**Figure S8.** ORTEP drawing of **2a•THF** with 30% thermal ellipsoids. H atoms are omitted for clarity.

**Table S1 Crystal data and structure refinement for 2a•THF.**

Identification code	<b>2a•THF</b>
Empirical formula	$C_{58}H_{100}I_3LiO_9Si_2Sm_2$
Formula weight	1685.89
Temperature/K	100.01(10)
Crystal system	monoclinic
Space group	Cc
a/Å	12.2283(3)
b/Å	22.3914(4)
c/Å	25.1344(5)
$\alpha/^\circ$	90
$\beta/^\circ$	97.7741(19)
$\gamma/^\circ$	90
Volume/Å <sup>3</sup>	6818.8(2)
Z	4
$\rho_{\text{calc}}/\text{cm}^3$	1.642
$\mu/\text{mm}^{-1}$	3.146
F(000)	3336.0
Crystal size/mm <sup>3</sup>	0.1 × 0.1 × 0.05
Radiation	MoK $\alpha$ ( $\lambda$ = 0.71073)
2 $\theta$ range for data collection/ $^\circ$	7.176 to 50.05
Index ranges	-14 ≤ h ≤ 14, -26 ≤ k ≤ 26, -29 ≤ l ≤ 29
Reflections collected	114197
Independent reflections	11821 [ $R_{\text{int}}$ = 0.0581, $R_{\text{sigma}}$ = 0.0264]
Data/restraints/parameters	11821/2/682
Goodness-of-fit on $F^2$	1.071
Final R indexes [ $I \geq 2\sigma(I)$ ]	$R_1$ = 0.0213, $wR_2$ = 0.0503
Final R indexes [all data]	$R_1$ = 0.0223, $wR_2$ = 0.0507
Largest diff. peak/hole / e Å <sup>-3</sup>	0.94/-0.34
Flack parameter	-0.025(4)

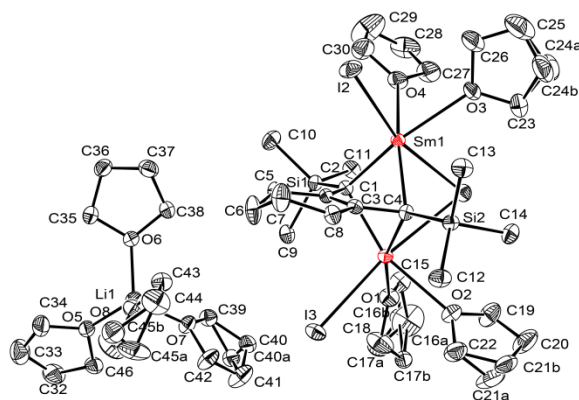


**Figure S9.** ORTEP drawing of **2c** with 30% thermal ellipsoids. H atoms are omitted for clarity.

**Table S2 Crystal data and structure refinement for 2c.**

Identification code	<b>2c</b>
Empirical formula	$\text{C}_{46}\text{H}_{90}\text{I}_3\text{LiO}_8\text{Si}_2\text{Sm}_2$
Formula weight	1515.69
Temperature/K	179.99(10)
Crystal system	monoclinic
Space group	$P2_1/c$
$a/\text{\AA}$	21.1690(4)
$b/\text{\AA}$	13.4380(3)
$c/\text{\AA}$	23.0935(5)
$\alpha/^\circ$	90
$\beta/^\circ$	99.119(2)
$\gamma/^\circ$	90
Volume/ $\text{\AA}^3$	6486.4(2)
Z	4
$\rho_{\text{calc}}/\text{mg}/\text{mm}^3$	1.552
$\mu/\text{mm}^{-1}$	3.297
F(000)	2976
Crystal size/ $\text{mm}^3$	$0.15 \times 0.1 \times 0.1$
Radiation	MoK $\alpha$ ( $\lambda = 0.71073$ )
2 $\theta$ range for data collection	3.882 to 49.994 $^\circ$
Index ranges	$-25 \leq h \leq 25, -15 \leq k \leq 15, -27 \leq l \leq 27$
Reflections collected	107019
Independent reflections	11400 [ $R_{\text{int}} = 0.0424, R_{\text{sigma}} = 0.0221$ ]
Data/restraints/parameters	11400/60/620
Goodness-of-fit on $F^2$	1.039
Final R indexes [ $I \geq 2\sigma(I)$ ]	$R_1 = 0.0273, wR_2 = 0.0572$
Final R indexes [all data]	$R_1 = 0.0355, wR_2 = 0.0600$
Largest diff. peak/hole / $e \text{\AA}^{-3}$	1.11/-0.87



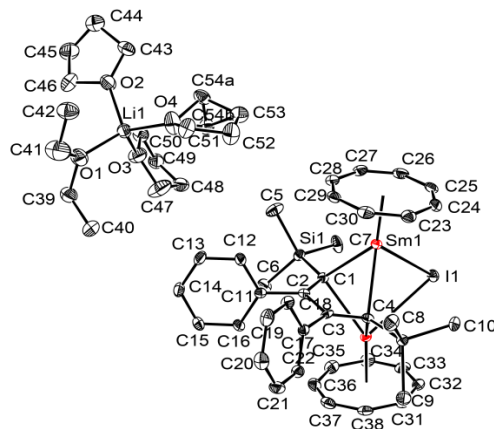


**Table S3 Crystal data and structure refinement for 3a.**

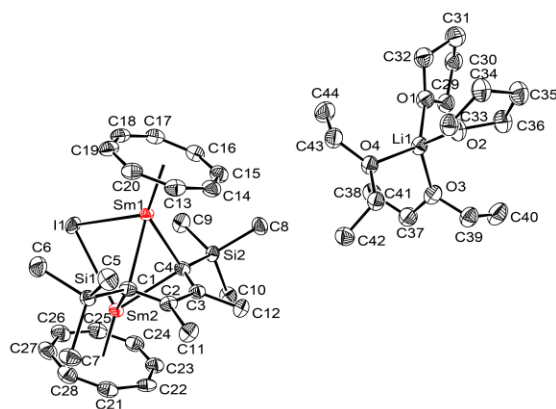


**Figure S11.** ORTEP drawing for one of two independent molecules of **3b** with 30% thermal ellipsoids. H atoms are omitted for clarity.

**Table S4 Crystal data and structure refinement for 3b.**

Identification code	<b>3b</b>
Empirical formula	$\text{C}_{44}\text{H}_{76}\text{ILiO}_4\text{Si}_2\text{Sm}_2$
Formula weight	1159.77
Temperature/K	180.00(10)
Crystal system	orthorhombic
Space group	$P2_12_12_1$
$a/\text{\AA}$	15.6548(2)
$b/\text{\AA}$	22.7462(3)
$c/\text{\AA}$	28.3983(4)
$\alpha/^\circ$	90.00
$\beta/^\circ$	90.00
$\gamma/^\circ$	90.00
Volume/ $\text{\AA}^3$	10112.3(2)
Z	8
$\rho_{\text{calc}}/\text{g cm}^{-3}$	1.524
$\mu/\text{mm}^{-1}$	2.993
$F(000)$	4640.0
Crystal size/ $\text{mm}^3$	$0.5 \times 0.3 \times 0.1$
Radiation	$\text{MoK}\alpha$ ( $\lambda = 0.71073$ )
$2\theta$ range for data collection/ $^\circ$	4.66 to 52.044
Index ranges	$-19 \leq h \leq 19, -27 \leq k \leq 28, -34 \leq l \leq 35$
Reflections collected	165156
Independent reflections	19824 [ $R_{\text{int}} = 0.0437$ , $R_{\text{sigma}} = 0.0267$ ]
Data/restraints/parameters	19824/3691/997
Goodness-of-fit on $F^2$	1.029
Final R indexes [ $I \geq 2\sigma(I)$ ]	$R_1 = 0.0348$ , $wR_2 = 0.0874$
Final R indexes [all data]	$R_1 = 0.0393$ , $wR_2 = 0.0898$
Largest diff. peak/hole / $e \text{\AA}^{-3}$	1.42/-0.90

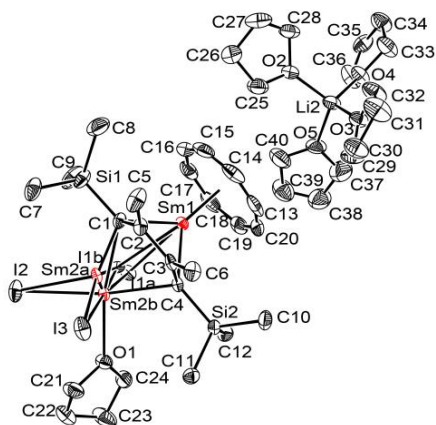


**Figure S12.** ORTEP drawing of **3b'** with 30% thermal ellipsoids. H atoms are omitted for clarity.

**Table S5 Crystal data and structure refinement for 3b'.**

Identification code	<b>3b'</b>
Empirical formula	C <sub>40</sub> H <sub>72</sub> I <sub>3</sub> LiO <sub>5</sub> Si <sub>2</sub> Sm <sub>2</sub>
Formula weight	1377.49
Temperature/K	179.99(10)
Crystal system	monoclinic
Space group	P2 <sub>1</sub> /n
a/Å	22.5968(4)
b/Å	9.5025(2)
c/Å	24.1613(5)
α/°	90.00
β/°	91.482(2)
γ/°	90.00
Volume/Å <sup>3</sup>	5186.33(18)
Z	4
ρ <sub>calc</sub> /g/cm <sup>3</sup>	1.764
μ/mm <sup>-1</sup>	4.109
F(000)	2664.0
Crystal size/mm <sup>3</sup>	0.5 × 0.4 × 0.1
Radiation	MoKα (λ = 0.71073)
2θ range for data collection/°	5.32 to 50
Index ranges	-26 ≤ h ≤ 26, -11 ≤ k ≤ 11, -28 ≤ l ≤ 28
Reflections collected	86224
Independent reflections	9131 [R <sub>int</sub> = 0.0394, R <sub>sigma</sub> = 0.0208]
Data/restraints/parameters	9131/84/505
Goodness-of-fit on F <sup>2</sup>	1.156
Final R indexes [I ≥ 2σ (I)]	R <sub>1</sub> = 0.0350, wR <sub>2</sub> = 0.0785
Final R indexes [all data]	R <sub>1</sub> = 0.0374, wR <sub>2</sub> = 0.0793
Largest diff. peak/hole / e Å <sup>-3</sup>	1.21/-1.75

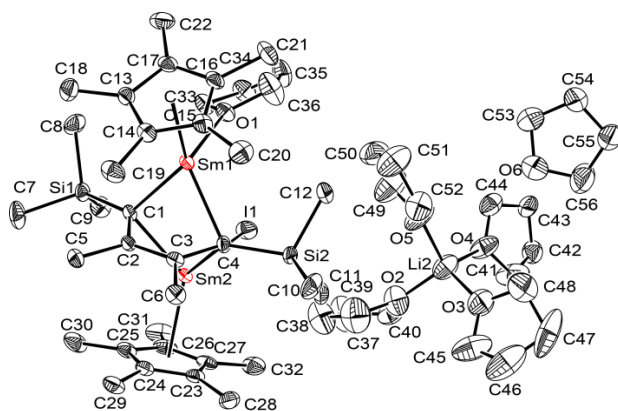


**Figure S13.** ORTEP drawing of **4b•THF** with 30% thermal ellipsoids. H atoms are omitted for clarity.

**Table S6 Crystal data and structure refinement for 4b•THF.**

Identification code	<b>4b•THF</b>
Empirical formula	$C_{56}H_{102}ILiO_6Si_2Sm_2$
Formula weight	1362.09
Temperature/K	179.99(10)
Crystal system	monoclinic
Space group	$P2_1/c$
$a/\text{\AA}$	16.8580(3)
$b/\text{\AA}$	10.9203(2)
$c/\text{\AA}$	34.7768(5)
$\alpha/^\circ$	90
$\beta/^\circ$	97.6680(10)
$\gamma/^\circ$	90
Volume/ $\text{\AA}^3$	6344.96(19)
Z	4
$\rho_{\text{calc}}/\text{g cm}^{-3}$	1.426
$\mu/\text{mm}^{-1}$	2.399
$F(000)$	2776.0
Crystal size/ $\text{mm}^3$	$0.3 \times 0.1 \times 0.1$
Radiation	MoK $\alpha$ ( $\lambda = 0.71073$ )
$2\theta$ range for data collection/ $^\circ$	4.416 to 49.998
Index ranges	$-18 \leq h \leq 20, -12 \leq k \leq 12, -41 \leq l \leq 41$
Reflections collected	79508
Independent reflections	11058 [ $R_{\text{int}} = 0.0323, R_{\text{sigma}} = 0.0203$ ]
Data/restraints/parameters	11058/21/631
Goodness-of-fit on $F^2$	1.167
Final R indexes [ $I \geq 2\sigma(I)$ ]	$R_1 = 0.0390, wR_2 = 0.0827$
Final R indexes [all data]	$R_1 = 0.0455, wR_2 = 0.0847$
Largest diff. peak/hole / $e \text{\AA}^{-3}$	1.00/-0.85



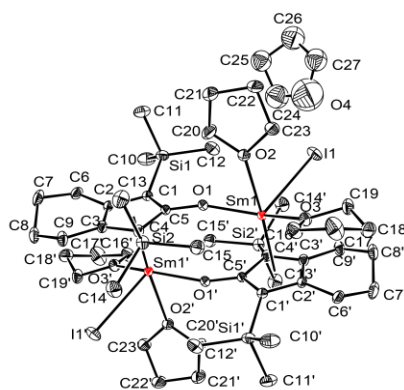


**Figure S15.** ORTEP drawing of one of two repeating molecules of **5c•THF** with 30% thermal ellipsoids. H atoms are omitted for clarity.

**Table S8 Crystal data and structure refinement for 5c•THF.**

Identification code	<b>5c•THF</b>
Empirical formula	C <sub>27</sub> H <sub>50</sub> IO <sub>4</sub> Si <sub>2</sub> Sm
Formula weight	772.10
Temperature/K	180.00(10)
Crystal system	triclinic
Space group	P-1
a/Å	11.7202(4)
b/Å	12.2687(4)
c/Å	13.6693(4)
α/°	114.227(3)
β/°	99.399(3)
γ/°	109.187(3)
Volume/Å <sup>3</sup>	1588.17(9)
Z	2
ρ <sub>calc</sub> /cm <sup>3</sup>	1.615
μ/mm <sup>-1</sup>	2.924
F(000)	774.0
Crystal size/mm <sup>3</sup>	0.05 × 0.05 × 0.05
Radiation	MoKα (λ = 0.71073)
2θ range for data collection/°	5.04 to 60.74
Index ranges	-15 ≤ h ≤ 16, -17 ≤ k ≤ 16, -18 ≤ l ≤ 18
Reflections collected	32827
Independent reflections	8298 [R <sub>int</sub> = 0.0379, R <sub>sigma</sub> = 0.0334]
Data/restraints/parameters	8298/38/322
Goodness-of-fit on F <sup>2</sup>	1.034
Final R indexes [I ≥ 2σ (I)]	R <sub>1</sub> = 0.0327, wR <sub>2</sub> = 0.0815
Final R indexes [all data]	R <sub>1</sub> = 0.0432, wR <sub>2</sub> = 0.0894
Largest diff. peak/hole / e Å <sup>-3</sup>	1.81/-0.93

#### 4) UV-Vis Spectrum and Magnetic Susceptibility of **2**

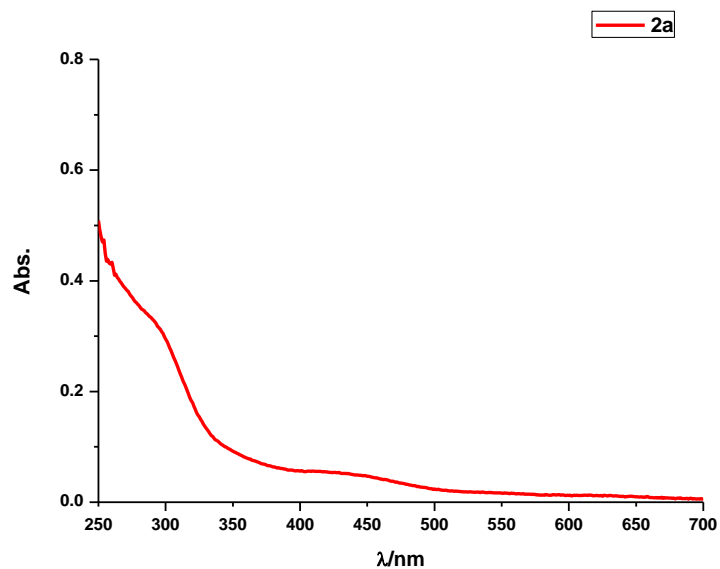


**Figure S16.** UV-Vis absorption spectrum of **2a** in THF (ca.  $3 \times 10^{-5}$  M) at 298 K.

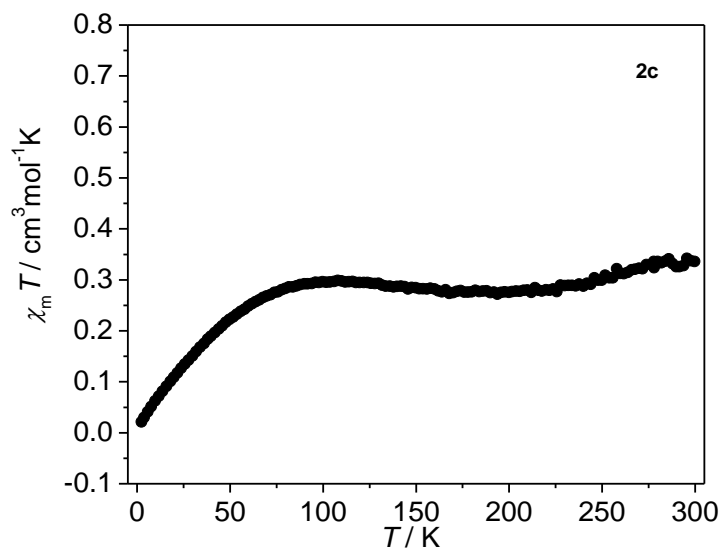


**Figure S17.** Variable-field  $\chi_m T$  vs  $T$  plots for **2c**.

## 5) Details of DFT Calculations

The theoretical calculations were carried out using the Amsterdam Density Functional Program (ADF 2019.102) with the B3LYP functional<sup>6,7</sup> and the Slater-type orbital (STO) basis sets of triple-zeta quality plus two polarization functions (TZ2P).<sup>8</sup> The frozen core approximation was applied to the  $[1s^2-4d^{10}]$  cores of Sm,  $[1s^2-4p^6]$  cores of I and  $[1s^2]$  cores of Si and C. The scalar relativistic (SR) effects were taken into consideration by the zeroth-order regular approximation (ZORA).<sup>9-11</sup> All the geometries were fully optimized using these computational selections. The effect of solvent was considered by employing the Minnesota's Solvation Model 12 (SM12) when calculating the single point energies of the intermediates in the reaction mechanism.<sup>12</sup> THF was used as the solvent. The high spin states were used for calculations since the spin multiplicity arises from f-orbitals do not have significant effect on the geometry and bonding in our cases. The energy decomposition analysis with natural orbitals for chemical valence (EDA-NOCV)<sup>13,14</sup> was performed based on the above geometry at B3LYP/TZ2P level. All the reported results by ADF 2019.02 are from 4f-in-valence calculations.

The single point calculations based on geometries optimized above were performed for further bonding analyses in Gaussian 16 with the same B3LYP functional.<sup>15</sup> The Stuttgart energy-consistent pseudo-potentials and their optimized basis sets were utilized for 4f-in-core Sm(ECP51MWB) and I(ECP46MWB).<sup>16-18</sup> Def2TZVP basis set was used for all the other light elements.<sup>19</sup> Both 4f-in-core and 4f-in-valence (ECP28MWB\_SEG)<sup>20,21</sup> pseudo-potentials of Sm were adopted to compare the role of Sm 4f orbitals. The reported results calculated by Gaussian 16 are from 4f-in-core unless specified otherwise. The adaptive natural density partitioning (AdNDP)<sup>22</sup> and the principal interacting orbital (PIO)<sup>23</sup> were used based on the single point calculations for chemical bonding analyses. The package Jmol was employed for visualization.<sup>24</sup> The AdNDP orbital composition was evaluated using Multiwfn by natural atomic orbital (NAO).<sup>25,26</sup>

### 5.1 Calculations on the Structures of 2 and 3

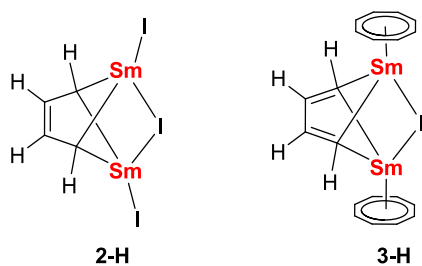


**Figure S18.** The simplified models **2-H** and **3-H**.



**Table S9.** The selected bond lengths (Å) of optimized geometry **2a** and simplified model **2-H** based on DFT optimization (B3LYP) as well as the corresponding experimentally measured ones.

Distance	Exp.	Calc.	
	<b>2a</b>	<b>2a</b>	<b>2-H</b>
C1-C2	1.463(8)	1.462	1.452
C2-C3	1.448(8)	1.439	1.422
C3-C4	1.468(8)	1.462	1.452
Sm1-C1	2.400(6)	2.349	2.391
Sm1-C2	2.689(7)	2.668	2.677
Sm1-C3	2.671(6)	2.668	2.677
Sm1-C4	2.380(6)	2.349	2.391
Sm2-C1	2.385(6)	2.349	2.391
Sm2-C2	2.671(6)	2.668	2.677
Sm2-C3	2.681(6)	2.668	2.677
Sm2-C4	2.404(6)	2.349	2.391
Sm1-I1	3.1437(5)	3.099	3.109
Sm1-I2	3.4022(5)	3.259	3.276
Sm2-I2	3.2268(5)	3.259	3.276
Sm2-I3	3.1688(6)	3.099	3.109

**Table S10.** The selected bond lengths (Å) of optimized geometry **3a** and simplified model **3-H** based on DFT optimization (B3LYP) as well as the corresponding experimentally measured ones.

Distance	Exp.	Calc.	
	<b>3a</b>	<b>3a</b>	<b>3-H</b>
C1-C2	1.355(10)	1.371	1.364
C2-C3	1.562(9)	1.532	1.483
C3-C4	1.383(10)	1.371	1.364
Sm1-C1	2.580(7)	2.654	2.609
Sm1-C4	2.603(7)	2.654	2.609
Sm2-C1	2.592(7)	2.654	2.609
Sm2-C4	2.598(7)	2.654	2.609
Sm1-I1	3.2145(6)	3.240	3.269
Sm2-I2	3.2253(6)	3.240	3.269

**Table S11.** The selected bond distance (Å) and the corresponding Mayer bond orders<sup>27</sup> for the selected bond lengths of **2a** and **3a**.

Distance	<b>2a</b>			<b>3a</b>		
	Exp.	Calc.	Mayer BO	Exp.	Calc.	Mayer BO
C1-C2	1.463(8)	1.462	0.96	1.355(10)	1.371	1.71
C2-C3	1.448(8)	1.439	1.32	1.562(9)	1.532	1.07
C3-C4	1.468(8)	1.462	0.96	1.383(10)	1.371	1.71
Sm1-C1	2.400(6)	2.349	0.61	2.580(7)	2.654	0.24
Sm1-C2	2.689(7)	2.668	0.14	--	3.099	0.03

**Table S12a.** AdNDP orbital compositions evaluated by the natural atomic orbital (NAO) method of simplified model **2-H** from 4f-in-core calculations. The contribution less than 0.5% is not listed.

Orb.	Sm1+Sm2	C1	C2	C3	C4
$\sigma_1$	16.4%(s <sup>0.15</sup> d)	83.6%(s <sup>0.67</sup> p)	--	--	--
$\sigma_2$	16.4%(s <sup>0.15</sup> d)	--	--	--	83.6%(s <sup>0.67</sup> p)
$\pi_1$	6.3%(s <sup>0.60</sup> d)	19.1%(p)	27.7%(p)	27.7%(p)	19.1%(p)
$\pi_2$	10.9%(d)	32.2%(p)	12.4%(p)	12.4%(p)	32.2%(p)
$\pi_3^*$	29.4%(s <sup>0.10</sup> d)	17.5%(p)	17.8%(p)	17.8%(p)	17.5%(p)

**Table S12b.** AdNDP orbital compositions evaluated by the natural atomic orbital (NAO) method of simplified model **2-H** from 4f-in-valence calculations. The contribution less than 0.5% is not listed.

Orb.	Sm1+Sm2	C1	C2	C3	C4
$\sigma_1$	19.1% (s <sup>0.17</sup> df <sup>0.22</sup> )	80.9% (s <sup>0.62</sup> p)	--	--	--
$\sigma_2$	19.1% (s <sup>0.17</sup> df <sup>0.22</sup> )	--	--	--	80.9% (s <sup>0.62</sup> p)
$\pi_1$	4.3% (s <sup>0.44</sup> d)	10.4% (p)	37.5% (p)	37.5% (p)	10.4% (p)
$\pi_2$	11.4% (d)	31.4% (p)	12.9% (p)	12.9% (p)	31.4% (p)
$\pi_3^*$	42.7% (s <sup>0.10</sup> d <sup>0.52</sup> f)	22.3% (p)	6.4% (p)	6.4% (p)	22.3% (p)

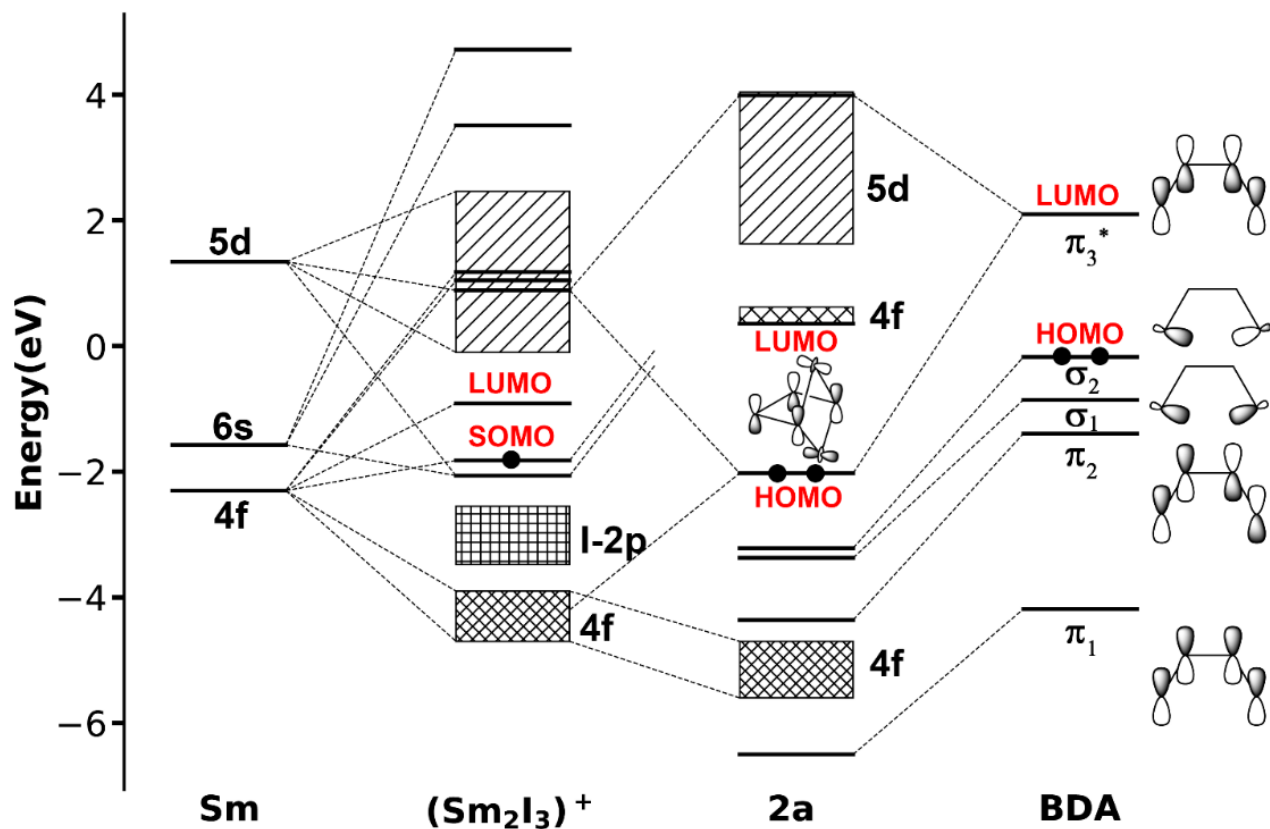
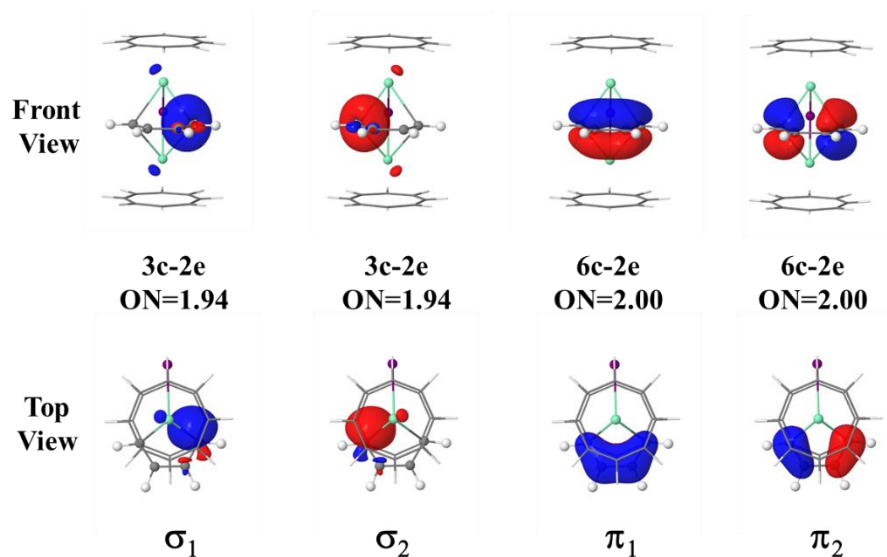


**Figure S19.** Kohn–Sham MO energy levels (B3LYP/TZ2P) of **2a**, illustrating the orbital interaction between the two fragments, 1,3-butadienyl dianions (BDA) and (Sm<sub>2</sub>I<sub>3</sub>)<sup>+</sup>. From 4f-in-valence calculations the atomic orbitals (AOs) contributions of HOMO are 12% from Sm-f, 20% from Sm-d and 53% from C-p. The orbitals of iodine atoms in **2a** are not displayed for clarity.

a)



b)

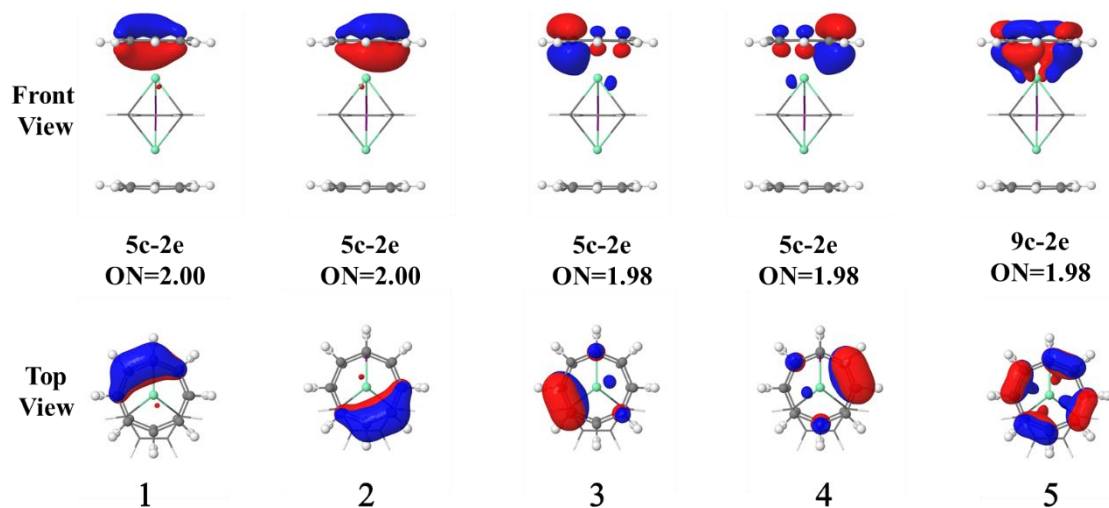


**Figure S20.** AdNDP orbitals and the occupation number (ON) of simplified model **3-H**. a) AdNDP bonds between the samarium atoms and the butadiene ligand. b) AdNDP bonds between the COT<sup>2-</sup> Ring and a samarium atom. Isovalue = 0.05.

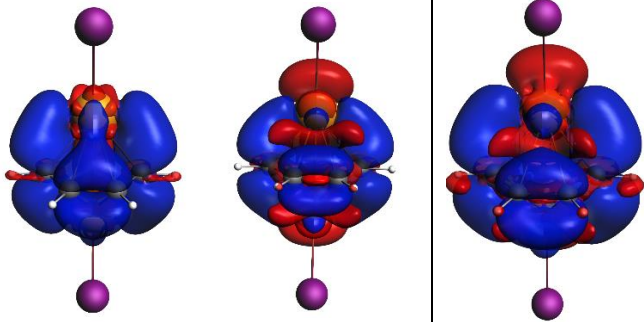
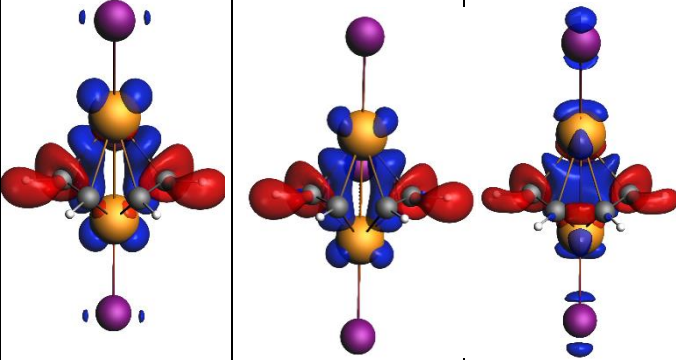
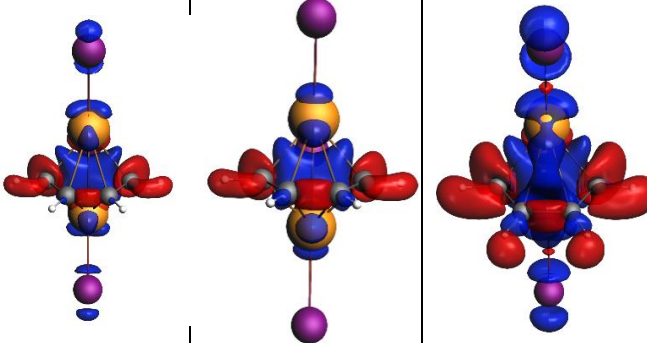
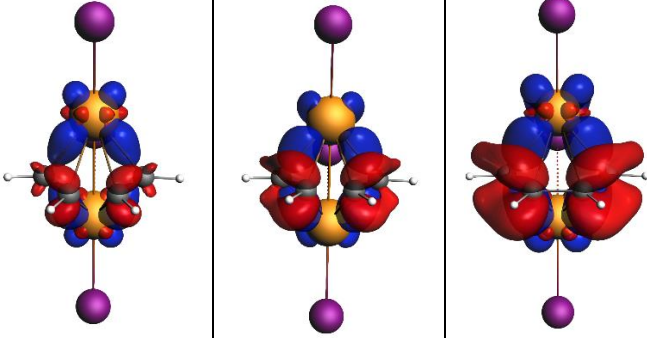
**Table S13.** AdNDP orbital compositions evaluated by the natural atomic orbital (NAO) method of simplified model **3-H**. The contribution less than 0.5% is not listed.

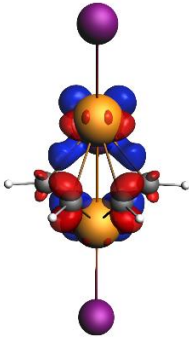
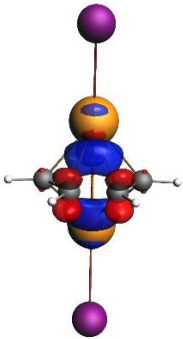
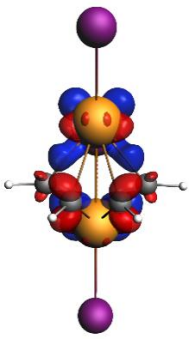
Orb.	Sm1+Sm2	C1	C2	C3	C4
$\sigma_1$	15.4%(s <sup>0.21</sup> d)	84.6%(s <sup>0.76</sup> p)	--	--	--
$\sigma_2$	15.4%(s <sup>0.21</sup> d)	--	--	--	84.6%(s <sup>0.76</sup> p)
$\pi_1$	2.3%(d)	14.9%(p)	34.0%(p)	34.0%(p)	14.9%(p)
$\pi_2$	4.8%(d)	32.3%(p)	15.3%(p)	15.3%	32.3%(p)

Orb.	Sm1/2	C(COT <sup>2-</sup> )
1	6.3%(d)	93.7%(p)
2	6.3%(d)	93.7%(p)
3	5.5%(d)	94.5%(p)
4	5.5%(d)	94.5%(p)
5	10.6%(d)	89.4%(p)

**Table S14.** Energy decomposition analysis of **2-H** at the PBE/TZ2P level and the associated deformation densities  $\Delta\rho$  of the most important pairwise orbital interactions  $\Delta E_{\text{orb}}$  (Isosurfaces = 0.001 au). The direction of the charge flow is red to blue. Energy values are given in kcal•mol<sup>-1</sup>.

fragments	Sm <sub>2</sub> I <sub>3</sub> <sup>+</sup> : f <sup>11</sup> s <sup>β</sup> C <sub>4</sub> H <sub>4</sub> <sup>2-</sup> : <sup>1</sup> A <sub>1</sub>		
$\Delta E_{\text{int}}$	-476.60		
$\Delta E_{\text{Pauli}}$	765.33		
$\Delta E_{\text{elstat}}$	-781.96 (62.94%)		
$\Delta E_{\text{orb}}$	-460.30 (37.05%)		
	$\alpha$	$\beta$	$\alpha + \beta$

$\Delta E_{\text{orb}}(\pi_3^*)$			
	-44.60	-179.36	-223.96(48.65%)
$\Delta E_{\text{orb}}(\sigma)$			
	-36.03	-30.48	-66.51(14.45%)
$\Delta E_{\text{orb}}(\sigma)$			
	-25.50	-22.70	-48.20(10.47%)
$\Delta E_{\text{orb}}(\pi_2)$			

	-12.62	-19.20	-31.82(6.91%)
$\Delta E_{\text{orb}}(\pi_1)$			
	-9.08	-6.77	-15.85(3.44%)
$E_{\text{bonding}}$	470.01		

<sup>a</sup>The value in parentheses gives the percentage contribution to the total attractive interactions  $\Delta E_{\text{elstat}} + \Delta E_{\text{orb}}$ . <sup>b</sup>The value in parentheses gives the percentage contribution to the total orbital interactions  $\Delta E_{\text{orb}}$ . <sup>c</sup> $\Delta E_{\text{tot-bonding}} = \Delta E_{\text{prep}} + \Delta E_{\text{int}}$ .

The total interaction energies ( $\Delta E_{\text{int}}$ ) were decomposed into three terms, which are the electrostatic interaction energy ( $\Delta E_{\text{elstat}}$ ), Pauli repulsion ( $\Delta E_{\text{pauli}}$ ) and orbital interactions ( $\Delta E_{\text{orb}}$ ). The sum of the  $\Delta E_{\text{pauli}}$  and  $\Delta E_{\text{elstat}}$  is also called steric interactions ( $\Delta E_{\text{steric}}$ ). The EDA-NOCV calculations indicate that  $\Delta E_{\text{elstat}}$  is the dominant attractive forces in **2-H** and accounts for 63%, indicating the compounds are primarily stabilized by ionic interaction. The rest 37% orbital interaction also plays an important role since Pauli repulsion and electrostatic interaction almost cancel out. The breakdown of the orbital interaction term into individual orbital contributions reveals that the five components contribute 48.7% ( $\pi_3^*$ ), 24.9% (two  $\sigma$ ), 6.9% ( $\pi_2$ ) and a weaker 3.4% ( $\pi_1$ ), respectively. The  $\pi$  orbitals have the dominate contribution while the  $\sigma$  orbitals are also non-negligible. The deformation densities  $\Delta\rho(\sigma)$  and  $\Delta\rho(\pi)$  show the direction of the charge flow and the orbitals that are involved, where the color code of the charge flow is red  $\rightarrow$  blue. The charge flow clearly shows that not only C1 and C4 but also farther C2 and C3 are involved in the interaction between the metal ions and the butadienyl ligand.



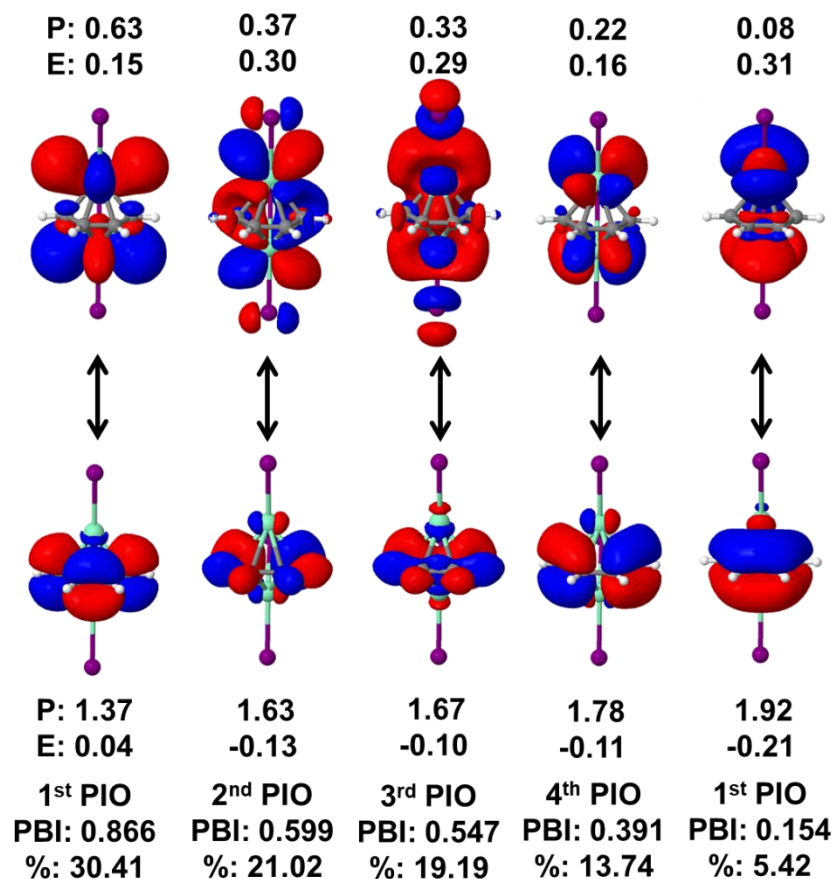


**Figure S21.** Results of PIO analysis on **2-H** with  $\text{Sm}_2\text{I}_3$  and  $\text{C}_4\text{H}_4$  as two fragments based on the B3LYP calculations with Stuttgart energy-consistent pseudo-potentials and their optimized basis sets for  $\text{Sm}(\text{ECP51MWB})$  and  $\text{I}(\text{ECP46MWB})$  and def2TZVP for the other elements. (a) The top five PIOs of each fragment. The orbital energies and populations (occupation numbers) are given as E and P, respectively, near each PIO. Given below each PIO pair are the PIO-based bond indices (abbreviated as PBI) and its contribution (as %) to the total interactions between two fragments (the contributions of all PIOs sum up to 100%). Isovalue: 0.02 for all orbitals.

## Calculated Energies and Geometrical Coordinates of Optimized Geometry 2a

Spin multiplicity: 11-et Energy = -9173.6 kcal/mol

Sm	0.000000	-1.688584	-0.785703
Sm	0.000000	1.688584	-0.785703
I	0.000000	-4.606155	0.259577
I	0.000000	0.000000	-3.573471
I	0.000000	4.606155	0.259577
Si	3.272349	0.000000	-0.520502
Si	-3.272349	0.000000	-0.520502
C	1.480046	0.000000	-0.097508
C	0.719560	0.000000	1.151153
C	-0.719560	0.000000	1.151153
C	-1.480046	0.000000	-0.097508
C	3.693602	-1.517347	-1.594257
H	3.541881	-2.453184	-1.044911
H	4.741535	-1.492093	-1.915381
H	3.079750	-1.548056	-2.501375
C	4.511848	0.000000	0.914127
H	4.397555	0.881403	1.550282
H	5.531836	0.000000	0.512216
H	4.397555	-0.881403	1.550282
C	3.693602	1.517347	-1.594257
H	3.079750	1.548056	-2.501375
H	4.741535	1.492093	-1.915381
H	3.541881	2.453184	-1.044911
C	-4.511848	0.000000	0.914127
H	-4.397555	-0.881403	1.550282
H	-5.531836	0.000000	0.512216
H	-4.397555	0.881403	1.550282
C	-3.693602	1.517347	-1.594257
H	-3.541881	2.453184	-1.044911
H	-4.741535	1.492093	-1.915381
H	-3.079750	1.548056	-2.501375
C	-3.693602	-1.517347	-1.594257
H	-3.079750	-1.548056	-2.501375

H	-4.741535	-1.492093	-1.915381
H	-3.541881	-2.453184	-1.044911
C	1.443965	0.000000	2.473717
C	1.806505	-1.204345	3.093759
H	1.534728	-2.147671	2.629459
C	2.507066	-1.205808	4.301330
H	2.773182	-2.150279	4.766071
C	2.861463	0.000000	4.910501
H	3.405686	0.000000	5.849801
C	2.507066	1.205808	4.301330
H	2.773182	2.150279	4.766071
C	1.806505	1.204345	3.093759
H	1.534728	2.147671	2.629459
C	-1.443965	0.000000	2.473717
C	-1.806505	-1.204345	3.093759
H	-1.534728	-2.147671	2.629459
C	-2.507066	-1.205808	4.301330
H	-2.773182	-2.150279	4.766071
C	-2.861463	0.000000	4.910501
H	-3.405686	0.000000	5.849801
C	-2.507066	1.205808	4.301330
H	-2.773182	2.150279	4.766071
C	-1.806505	1.204345	3.093759
H	-1.534728	2.147671	2.629459

### Calculated Energies and Geometrical Coordinates of Simplified Model 2-H

Spin multiplicity: 11-et Energy = -2371.5 kcal/mol

Sm	-1.691300	0.000000	0.784462
Sm	1.691300	0.000000	0.784462
I	-4.747262	0.000000	0.232533
I	0.000000	0.000000	3.569991
I	4.747262	0.000000	0.232533
C	0.000000	1.499630	0.074106
C	0.000000	0.713648	-1.146054
C	0.000000	-0.713648	-1.146054

C	0.000000	-1.499630	0.074106
H	0.000000	1.181627	-2.131262
H	0.000000	2.585328	-0.024472
H	0.000000	-1.181627	-2.131262
H	0.000000	-2.585328	-0.024472

### Calculated Energies and Geometrical Coordinates of Optimized Geometry 3a

Spin multiplicity: 11-et Energy = -14167.7 kcal/mol

Si	-3.355576	0.000000	0.057685
Si	3.355576	0.000000	0.057685
C	-1.465945	0.000000	0.209918
C	-0.765969	0.000000	1.388567
C	0.765969	0.000000	1.388567
C	1.465945	0.000000	0.209918
C	-4.220422	-1.502926	0.836139
H	-4.117980	-1.505611	1.923710
H	-5.289556	-1.453654	0.597924
H	-3.834559	-2.449142	0.454378
C	-4.220422	1.502926	0.836139
H	-3.834559	2.449142	0.454378
H	-5.289556	1.453654	0.597924
H	-4.117980	1.505611	1.923710
C	-3.804246	0.000000	-1.781016
H	-3.406041	-0.879145	-2.295665
H	-4.893096	0.000000	-1.904444
H	-3.406041	0.879145	-2.295665
C	4.220422	-1.502926	0.836139
H	5.289556	-1.453654	0.597924
H	4.117980	-1.505611	1.923710
H	3.834559	-2.449142	0.454378
C	4.220422	1.502926	0.836139
H	3.834559	2.449142	0.454378
H	4.117980	1.505611	1.923710
H	5.289556	1.453654	0.597924
C	3.804246	0.000000	-1.781016

H	3.406041	-0.879145	-2.295665
H	3.406041	0.879145	-2.295665
H	4.893096	0.000000	-1.904444
C	-1.430631	0.000000	2.747853
C	-1.754185	-1.203663	3.391996
H	-1.509531	-2.143952	2.909490
C	-2.388611	-1.205313	4.635429
H	-2.631526	-2.149914	5.112862
C	-2.709308	0.000000	5.263728
H	-3.201167	0.000000	6.231433
C	-2.388611	1.205313	4.635429
H	-2.631526	2.149914	5.112862
C	-1.754185	1.203663	3.391996
H	-1.509531	2.143952	2.909490
C	1.430631	0.000000	2.747853
C	1.754185	-1.203663	3.391996
H	1.509531	-2.143952	2.909490
C	2.388611	-1.205313	4.635429
H	2.631526	-2.149914	5.112862
C	2.709308	0.000000	5.263728
H	3.201167	0.000000	6.231433
C	2.388611	1.205313	4.635429
H	2.631526	2.149914	5.112862
C	1.754185	1.203663	3.391996
H	1.509531	2.143952	2.909490
Sm	0.000000	-1.886037	-0.947553
Sm	0.000000	1.886037	-0.947553
I	0.000000	0.000000	-3.581779
C	1.307782	3.945051	0.231192
H	2.073400	3.917055	1.001297
C	1.848086	3.857819	-1.073262
H	2.931560	3.783102	-1.072659
C	1.304974	3.799798	-2.380359
H	2.069306	3.669508	-3.141473
C	0.000000	3.788885	-2.917949
H	0.000000	3.638036	-3.993023

C	-1.304974	3.799798	-2.380359
H	-2.069306	3.669508	-3.141473
C	-1.848086	3.857819	-1.073262
H	-2.931560	3.783102	-1.072659
C	-1.307782	3.945051	0.231192
H	-2.073400	3.917055	1.001297
C	0.000000	3.983477	0.770509
H	0.000000	3.986790	1.857672
C	1.307782	-3.945051	0.231192
H	2.073400	-3.917055	1.001297
C	1.848086	-3.857819	-1.073262
H	2.931560	-3.783102	-1.072659
C	1.304974	-3.799798	-2.380359
H	2.069306	-3.669508	-3.141473
C	0.000000	-3.788885	-2.917949
H	0.000000	-3.638036	-3.993023
C	-1.304974	-3.799798	-2.380359
H	-2.069306	-3.669508	-3.141473
C	-1.848086	-3.857819	-1.073262
H	-2.931560	-3.783102	-1.072659
C	-1.307782	-3.945051	0.231192
H	-2.073400	-3.917055	1.001297
C	0.000000	-3.983477	0.770509
H	0.000000	-3.986790	1.857672

### Calculated Energies and Geometrical Coordinates of Simplified Model 3-H

Spin multiplicity: 11-et Energy = -7442.2 kcal/mol

C	-1.438823	0.000000	0.012631
C	-0.741270	0.000000	1.184417
C	0.741270	0.000000	1.184417
C	1.438823	0.000000	0.012631
Sm	0.000000	-1.866456	-1.107613
Sm	0.000000	1.866456	-1.107613
I	0.000000	0.000000	-3.791578
C	1.308945	3.760008	0.286324

H	2.070598	3.623030	1.049161
C	1.855458	3.810383	-1.017953
H	2.938062	3.716090	-1.022583
C	1.308905	3.904374	-2.322738
H	2.069534	3.855338	-3.096870
C	0.000000	3.957572	-2.854295
H	0.000000	3.926192	-3.940073
C	-1.308905	3.904374	-2.322738
H	-2.069534	3.855338	-3.096870
C	-1.855458	3.810383	-1.017953
H	-2.938062	3.716090	-1.022583
C	-1.308945	3.760008	0.286324
H	-2.070598	3.623030	1.049161
C	0.000000	3.750331	0.826136
H	0.000000	3.617421	1.904698
C	1.308945	-3.760008	0.286324
H	2.070598	-3.623030	1.049161
C	1.855458	-3.810383	-1.017953
H	2.938062	-3.716090	-1.022583
C	1.308905	-3.904374	-2.322738
H	2.069534	-3.855338	-3.096870
C	0.000000	-3.957572	-2.854295
H	0.000000	-3.926192	-3.940073
C	-1.308905	-3.904374	-2.322738
H	-2.069534	-3.855338	-3.096870
C	-1.855458	-3.810383	-1.017953
H	-2.938062	-3.716090	-1.022583
C	-1.308945	-3.760008	0.286324
H	-2.070598	-3.623030	1.049161
C	0.000000	-3.750331	0.826136
H	0.000000	-3.617421	1.904698
H	-2.527365	0.000000	0.127291
H	-1.214854	0.000000	2.172438
H	1.214854	0.000000	2.172438
H	2.527365	0.000000	0.127291

## 5.2 Calculations on the Proposed Mechanisms for the Formation of 2

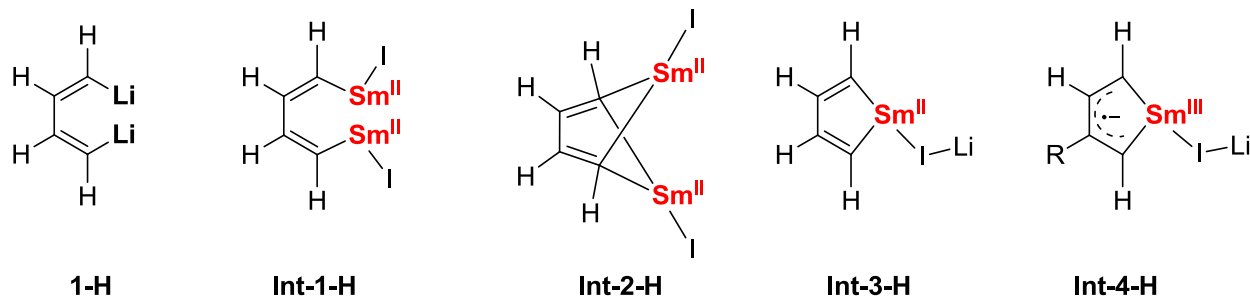


**Figure S22.** The simplified models for calculations.

**Table S15.** The relative energies of the intermediates in pathway-a and pathway-b calculated using DFT. The energies with effect of solvent THF considered by single-point solvation model 12 (SM12) are listed in brackets.

Pathway-a		Pathway-b	
Species	$\Delta E/(\text{kcal}\cdot\text{mol}^{-1})$	Species	$\Delta E/(\text{kcal}\cdot\text{mol}^{-1})$
<b>1-H</b> +2SmI <sub>2</sub>	0	<b>1-H</b> +2SmI <sub>2</sub>	0
<b>Int-1-H</b> +2LiI	-43.8 (-31.5)	<b>Int-3-H</b> +LiI+SmI <sub>2</sub>	-31.0 (-23.2)
<b>Int-2-H</b> +2LiI	-33.0 (-21.0)	<b>Int-4-H</b> +LiI+SmI <sub>2</sub>	+20.0 (+9.4)

### Calculated Energies and Geometrical Coordinates of Simplified Model 1-H

Spin multiplicity: singlet    Energy = -1297.2 kcal/mol

Li	1.822700	0.000000	1.538328
Li	-1.822700	0.000000	1.538328
C	-1.639454	0.000000	-0.397567
C	-0.742885	0.000000	-1.414356
C	0.742885	0.000000	-1.414356
C	1.639454	0.000000	-0.397567
H	2.663571	0.000000	-0.815068
H	1.125783	0.000000	-2.443469
H	-1.125783	0.000000	-2.443469
H	-2.663571	0.000000	-0.815068



### Calculated Energies and Geometrical Coordinates of Simplified Model Int-1-H

Spin multiplicity: 13-et Energy = -2171.2 kcal/mol

Sm	1.683605	0.000000	1.813518
Sm	-1.683605	0.000000	1.813518
I	0.000000	-2.383914	3.047253
I	0.000000	2.383914	3.047253
C	-1.547642	0.000000	-0.466565
C	-0.724083	0.000000	-1.564066
C	0.724083	0.000000	-1.564066
C	1.547642	0.000000	-0.466565
H	2.626908	0.000000	-0.747607
H	1.163831	0.000000	-2.565343
H	-1.163831	0.000000	-2.565343
H	-2.626908	0.000000	-0.747607

### Calculated Energies and Geometrical Coordinates of Simplified Model Int-2-H

Spin multiplicity: 13-et Energy = -2217.4 kcal/mol

Sm	0.000000	-1.745978	-0.701184
Sm	0.000000	1.745978	-0.701184
I	0.000000	-3.592693	-3.062087
I	0.000000	3.592693	-3.062087
C	1.481127	0.000000	0.199793
C	0.727028	0.000000	1.389639
C	-0.727028	0.000000	1.389639
C	-1.481127	0.000000	0.199793
H	2.569596	0.000000	0.329984
H	-2.569596	0.000000	0.329984
H	1.195992	0.000000	2.379023
H	-1.195992	0.000000	2.379023

### Calculated Energies and Geometrical Coordinates of Simplified Model Int-3-H

Spin multiplicity: septet    Energy = -1740.6 kcal/mol

C	1.604797	0.000000	2.595259
C	0.751629	0.000000	3.658891
C	-0.751629	0.000000	3.658891
C	-1.604797	0.000000	2.595259
H	2.664288	0.000000	2.855597
H	-1.148271	0.000000	4.679903
H	1.148271	0.000000	4.679903
H	-2.664288	0.000000	2.855597
Sm	0.000000	0.000000	0.847352
I	0.000000	0.000000	-2.422328
Li	0.000000	0.000000	-4.957365

### Calculated Energies and Geometrical Coordinates of Simplified Model Int-4-H

Spin multiplicity: septet    Energy = -1721.0 kcal/mol

C	1.536101	0.000000	2.584108
C	0.727833	0.000000	3.713588
C	-0.727833	0.000000	3.713588
C	-1.536101	0.000000	2.584108
H	2.609367	0.000000	2.791780
H	-1.178365	0.000000	4.710845
H	1.178365	0.000000	4.710845
H	-2.609367	0.000000	2.791780
Sm	0.000000	0.000000	0.852106
I	0.000000	0.000000	-2.474665
Li	0.000000	0.000000	-4.931120

## 6) References

- (1) Dolomanov, O. V.; Bourhis, L. J.; Gildea, R. J.; Howard, J. A. K.; Puschmann, H. *OLEX2: A Complete Structure Solution, Refinement and Analysis Program. J. Appl. Cryst.* **2009**, *42*, 339–341.
- (2) (a) Palatinus, L.; Chapuis, G. SUPERFLIP - a Computer Program for the Solution of Crystal Structures by Charge Flipping in Arbitrary Dimensions. *J. Appl. Cryst.* **2007**, *40*, 786–790. (b) Palatinus, L.; van der Lee, A. Symmetry Determination Following Structure Solution in P1. *J. Appl. Cryst.* **2008**, *41*, 975–984. (c) Palatinus, L.; Prathapa, S. J.; van Smaalen, S. EDMA: a Computer Program for Topological Analysis of Discrete Electron Densities. *J. Appl. Cryst.* **2012**, *45*, 575–580.
- (3) Sheldrick, G. M. A Short History of *SHELX*. *Acta Cryst.* **2008**, *A64*, 112–122.
- (4) Sheldrick, G. M. Crystal Structure Refinement with *SHELXL*. *Acta Cryst.* **2015**, *C71*, 3–8.
- (5) Farrugia, L. J. WinGX and ORTEP for Windows: an update. *J. Appl. Cryst.* **2012**, *45*, 849–854.
- (6) te Velde, G.; Bickelhaupt, F. M.; Baerends, E. J.; Fonseca Guerra, C.; van Gisbergen, S. J. A.; Snijders, J. G.; Ziegler, T. Chemistry with ADF. *J. Comp. Chem.* **2001**, *22*, 931–967.
- (7) (a) Becke, A. D., Density-functional Exchange-energy Approximation with Correct Asymptotic Behavior. *Phys. Rev. A: At., Mol., Opt. Phys.* **1988**, *38*, 3098–3100. (b) Lee, C.; Yang, W.; Parr, R. G. Development of the Colle-Salvetti Correlation-Energy Formula into a Functional of the Electron Density. *Phys. Rev. B: Condens. Matter Mater. Phys.* **1988**, *37*, 785–789.
- (8) van Lenthe, E.; Baerends, E. J. Optimized Slater-Type Basis Sets for the Elements 1–118. *J. Comp. Chem.* **2003**, *24*, 1142–1156.
- (9) van Lenthe, E.; Baerends, E. J.; Snijders, J. G. Relativistic Regular Two-component Hamiltonians. *J. Chem. Phys.* **1993**, *99*, 4597–4610.
- (10) van Lenthe, E.; Baerends, E. J.; Snijders, J. G. Relativistic Total Energy Using Regular Approximations. *J. Chem. Phys.* **1994**, *101*, 9783–9792.
- (11) van Lenthe, E.; Ehlers, A.; Baerends, E. J. Geometry Optimizations in the Zero Order Regular Approximation for Relativistic Effects. *J. Chem. Phys.* **1999**, *110*, 8943–8953.
- (12) Marenich, A. V.; Cramer, C. J.; Truhlar, D. G., Generalized born solvation model SM12. *J. Chem. Theory Comput.* **2013**, *9*, 609–620.
- (13) Michalak, A.; Mitoraj, M.; Ziegler, T. Bond Orbitals from Chemical Valence Theory. *J. Phys. Chem. A* **2008**, *112*, 1933–1939.
- (14) Mitoraj, M. P.; Michalak, A.; Ziegler, T. A Combined Charge and Energy Decomposition Scheme for Bond Analysis. *J. Chem. Theory Comput.* **2009**, *5*, 962–975.

- (15) Frisch, M. J.; Trucks, G. W.; Schlegel, H. B.; Scuseria, G. E.; Robb, M. A.; Cheeseman, J. R.; Scalmani, G.; Barone, V.; Mennucci, B.; Petersson, G. A.; Nakatsuji, H.; Caricato, M.; Li, X.; Hratchian, H. P.; Izmaylov, A. F.; Bloino, J.; Zheng, G.; Sonnenberg, J. L.; Hada, M.; Ehara, M.; Toyota, K.; Fukuda, R.; Hasegawa, J.; Ishida, M.; Nakajima, T.; Honda, Y.; Kitao, O.; Nakai, H.; Vreven, T.; Montgomery, Jr., J. A.; Peralta, J. E.; Ogliaro, F.; Bearpark, M.; Heyd, J. J.; Brothers, E.; Kudin, K. N.; Staroverov, V. N.; Keith, T.; Kobayashi, R.; Normand, J.; Raghavachari, K.; Rendell, A.; Burant, J. C.; Iyengar, S. S.; Tomasi, J.; Cossi, M.; Rega, N.; Millam, J. M.; Klene, M.; Knox, J. E.; Cross, J. B.; Bakken, V.; Adamo, C.; Jaramillo, J.; Gomperts, R.; Stratmann, R. E.; Yazyev, O.; Austin, A. J.; Cammi, R.; Pomelli, C.; Ochterski, J. W.; Martin, R. L.; Morokuma, K.; Zakrzewski, V. G.; Voth, G. A.; Salvador, P.; Dannenberg, J. J.; Dapprich, S.; Daniels, A. D.; Farkas, O.; Foresman, J. B.; Ortiz, J. V.; Cioslowski, J.; Fox, D. J. Gaussian 16, Revision B.01. Gaussian, Inc., Wallingford CT, 2016.
- (16) Dolg, M.; Stoll, H.; Preuss, H. A Combination of Quasirelativistic Pseudopotential and Ligand Field Calculations for Lanthanoid Compounds. *Theor. Chim. Acta.* **1993**, 85, 441–450.
- (17) Dolg, M.; Stoll, H.; Savin, A.; Preuss, H. Energy-adjusted Pseudopotentials for the Rare Earth Elements. *Theor. Chim. Acta.* **1989**, 75, 173–194.
- (18) Stoll, H.; Metz, B.; Dolg, M. Relativistic Energy-Consistent Pseudopotentials — Recent Developments. *J. Comp. Chem.* **2002**, 23, 767–778.
- (19) Weigend, F.; Ahlrichs, R. Balanced Basis Sets of Split Valence, Triple Zeta Valence and Quadruple Zeta Valence Quality for H to Rn: Design and Assessment of Accuracy. *Phys. Chem, Chem, Phys.* **2005**, 7, 3297–3305.
- (20) Dolg, M.; Stoll, H.; Preuss, H. Energy-Adjusted Abinitio Pseudopotentials for the Rare Earth elements. *J. Chem. Phys.* **1989**, 90, 1730–1734.
- (21) Cao, X.; Dolg, M. Segmented Contraction Scheme for Small-Core Lanthanide Pseudopotential Basis Sets. *J. Mol. Struct.* **2002**, 581, 139–147.
- (22) Zubarev, D. Y.; Boldyrev, A. I. Developing Paradigms of Chemical Bonding: Adaptive Natural Density Partitioning. *Phys. Chem. Chem. Phys.* **2008**, 10, 5207–5217.
- (23) Zhang, J. X.; Sheong, F. K.; Lin, Z. Y. Unravelling Chemical Interactions with Principal Interacting Orbital Analysis. *Chem. - Eur. J.* **2018**, 24, 9639–9650.
- (24) Herráez, A. Biomolecules in the Computer: Jmol to the Rescue. *Biochem. Mol. Biol. Educ.* **2006**, 34, 255–261.
- (25) Lu, T.; Chen, F. Multiwfn: a Multifunctional Wavefunction Analyzer. *J. Comp. Chem.* **2012**, 33,

580–592.

(26) Lu, T.; Cheng, F. Calculation of Molecular Orbital Composition. *Acta. Chim. Sinica.* **2011**, 69, 2393–2406 (in Chinese).

(27) Mayer, I. Charge, Bond Order and Valence in the AB Initio SCF Theory. *Chem. Phys. Lett.* **1983**, 97, 270–274.